Return Augmented Decision Transformer for Off-Dynamics Reinforcement Learning

Ruhan Wang*   *ruhwang@iu.edu*
Indiana University

Yu Yang*   *yu.yang@duke.edu*
Duke University

Zhishuai Liu   *zhishuai.liu@duke.edu*
Duke University

Dongruo Zhou   *dz13@iu.edu*
Indiana University

Pan Xu   *pan.xu@duke.edu*
Duke University

Reviewed on OpenReview: *https://openreview.net/forum?id=QDVOr5J9Xp*

Abstract

We study offline off-dynamics reinforcement learning (RL) to utilize data from an easily accessible source domain to enhance policy learning in a target domain with limited data. Our approach centers on return-conditioned supervised learning (RCSL), particularly focusing on Decision Transformer (DT) type frameworks, which can predict actions conditioned on desired return guidance and complete trajectory history. Previous works address the dynamics shift problem by augmenting the reward in the trajectory from the source domain to match the optimal trajectory in the target domain. However, this strategy can not be directly applicable in RCSL owing to (1) the unique form of the RCSL policy class, which explicitly depends on the return, and (2) the absence of a straightforward representation of the optimal trajectory distribution. We propose the Return Augmented (REAG) method for DT type frameworks, where we augment the return in the source domain by aligning its distribution with that in the target domain. We provide the theoretical analysis demonstrating that the RCSL policy learned from REAG achieves the same level of suboptimality as would be obtained without a dynamics shift. We introduce two practical implementations $\text{REAG}^*_{\text{Dara}}$ and $\text{REAG}^*_{\text{MV}}$ respectively. Thorough experiments on D4RL datasets and various DT-type baselines demonstrate that our methods consistently enhance the performance of DT type frameworks in off-dynamics RL.

1 Introduction

Off-dynamics reinforcement learning (Eysenbach et al., 2020; Jiang et al., 2021; Liu et al., 2022; Liu & Xu, 2024; Guo et al., 2025) arises in decision-making domains such as autonomous driving (Pan et al., 2017) and medical treatment (Laber et al., 2018; Liu et al., 2023), where direct policy training through trial-and-error in the target environment is often costly, unethical, or infeasible. A common strategy is to train the policy in source environments with similar but more accessible dynamics. However, discrepancies between the source and target environments create a simulation-to-reality (sim-to-real) gap, which can lead to catastrophic failures when deploying the source-trained policy in the target environment.

---

*Equal contribution.

Beyond the challenge of dynamics shift, practical scenarios often do not allow real-time online interaction with the source environment due to time and computational constraints. As a result, policies must be learned from pre-collected datasets generated by behavior policies. This setting is particularly difficult, as it combines off-policy, offline, and off-dynamics characteristics. Recently, supervised learning–based methods (Chen et al., 2021; Brandfonbrener et al., 2022) have emerged as more stable and scalable alternatives to traditional offline reinforcement learning algorithms grounded in dynamic programming (Levine et al., 2020). In the offline off-dynamics setting, the majority of training data is drawn from the source domain, with only a limited portion collected from the target domain. Our study focuses on advancing Decision Transformer (DT) type frameworks (Chen et al., 2021; Hu et al., 2024; Zhuang et al., 2024) for off-dynamics reinforcement learning, which can be viewed as a special case of return-conditioned supervised learning (RCSL) (Emmons et al., 2021; Brandfonbrener et al., 2022). While DT-type methods have gained significant attention across various reinforcement learning tasks, no prior work has explicitly tackled the off-dynamics RL problem.

There are several previous significant works in off-dynamics reinforcement learning that employ reward augmentation to address the dynamics shift between source and target environments (Eysenbach et al., 2020; Liu et al., 2022). In particular, Eysenbach et al. (2020) proposed the DARC algorithm to train a policy in the source domain using augmented rewards. These augmentations are derived by minimizing the KL distance between the distribution of trajectories generated by the learning policy in the source domain and those generated by the optimal policy in the target domain. Liu et al. (2022) extended this idea to the offline setting with the DARA algorithm. However, these reward augmentation techniques for dynamic programming based RL algorithms are not directly applicable to RCSL methods for two primary reasons. First, the policy classes used in RCSL methods explicitly depend on the conditional return-to-go function, leading to different trajectory distributions that invalidate the trajectory matching methods. Second, the augmentation techniques in Eysenbach et al. (2020); Liu et al. (2022) explicitly rely on the form of the optimal trajectory distribution in the target domain. In contrast, there is no straightforward representation of the optimal RCSL policy and the trajectory distribution. Therefore, novel augmentation mechanisms must be derived for RCSL methods to effectively address off-dynamics reinforcement learning.

In this work, we propose the Return Augmented (REAG) algorithm, which augments the returns of trajectories from a source environment to better align with the target environment within DT-type frameworks. Through rigorous analysis, we show that the RCSL policy learned with REAG in the source domain achieves suboptimality comparable to that of a policy learned directly in the target domain without dynamics shift. Building upon our preliminary study on return augmentation for Decision Transformer (RADT)(Wang et al., 2024), the present work substantially generalizes and extends this idea by developing a unified REAG framework that integrates augmentation across multiple DT-type architectures, introduces practical stabilization mechanisms, and provides expanded empirical evaluation under structured dynamics shifts. Specifically, our contributions are summarized as follows:

- We propose a novel method, REAG, specifically designed for DT-type architectures in the off-dynamics RL setting. The approach augments the returns of offline trajectories in the source domain by leveraging a small amount of data from the target domain. We develop two practical implementations of REAG: $\text{REAG}^*_{\text{Dara}}$, derived from reward augmentation techniques used in dynamic programming–based methods, and $\text{REAG}^*_{\text{MV}}$ from direct return distribution matching.
- We provide a rigorous theoretical analysis demonstrating that the return-conditioned policy learned via REAG can achieve suboptimality comparable to that of a policy trained directly on the target domain. Our analysis relies on the same data coverage assumptions as Brandfonbrener et al. (2022), which consider the no dynamics shift setting. This result implies that return augmentation can enhance the performance of RCSL in off-dynamics reinforcement learning, particularly when the available source dataset is substantially larger than the target dataset..
- We conduct experiments on the D4RL benchmark by training policies on source datasets collected from modified dynamics and evaluating them in the original environments. Across DT-type baselines—including DT (Chen et al., 2021), Reinformer (Zhuang et al., 2024) and QT (Hu et al., 2024)—both $\text{REAG}^*_{\text{Dara}}$ and $\text{REAG}^*_{\text{MV}}$ consistently improve performance, with $\text{REAG}^*_{\text{MV}}$ showing the greatest gains, highlighting the advantage of return-level augmentation.

2 Related Work

Off-dynamics reinforcement learning (RL) is a specialized domain adaptation problem that draws inspiration from broader transfer learning principles (Pan & Yang, 2009). Numerous algorithms have been proposed to address the discrepancy between source and target environments (Niu et al., 2022; Liu et al., 2024; Xu et al., 2024; Gui et al., 2023; Lyu et al., 2024a;b). One promising approach involves modifying the reward function in the source domain. For instance, the DARC algorithm (Eysenbach et al., 2020) addresses this challenge in online settings by employing a reward augmentation method that aligns the optimal trajectory distributions of the source and target domains. Building on this, DARA (Liu et al., 2022) uses reward augmentation to supplement a limited target dataset with a larger source dataset in offline scenarios. However, a known limitation is that policies learned in the source domain often require an additional imitation learning step to effectively transfer behavior to the target domain (Guo et al., 2025). Unlike these dynamic programming-based methods, our work adopts the adaptation setting of DARA but introduces a novel augmentation method specifically designed for Return-Conditioned Supervised Learning (RCSL), with a particular focus on the Decision Transformer.

Another category of methods utilizes source data directly without augmentation, instead applying learned filtering mechanisms based on dynamics mismatch. Specifically, H2O (Niu et al., 2022) performs importance weighting to penalize Q-values associated with large dynamics gaps in offline-to-online transitions. VGDF (Xu et al., 2024) filters data based on value consistency in online scenarios, while CPD (Gui et al., 2023) utilizes a dynamics alignment module to minimize discrepancies. Additionally, PAR (Lyu et al., 2024a) addresses off-dynamics issues by capturing representation mismatches. Recent benchmarks (Lyu et al., 2024b) have also demonstrated that IQL maintains robust performance in off-dynamics settings. In the context of cross-domain offline RL, BOSA (Liu et al., 2024) tackles out-of-distribution (OOD) state-actions and dynamics through policy and value optimization, respectively. IGDF (Wen et al., 2024) selectively shares source domain transitions via contrastive learning, while SRPO (Xue et al., 2024) regularizes the policy using learned stationary state distributions. Most recently, MOBODY (Guo et al., 2026) proposed a model-based approach that learns a proxy for the target transition model through joint representation learning, subsequently using generated target data for policy optimization.

Return Conditioned Supervised Learning (RCSL) has emerged as a powerful framework for offline RL (Brandfonbrener et al., 2022). Notable implementations such as RvS (Emmons et al., 2021) and the Decision Transformer (DT) (Chen et al., 2021) have demonstrated performance competitive with traditional RL methods. The core principle of RCSL is to condition policies on a desired target return. In this paper, we focus on the Decision Transformer, which treats offline RL as a sequence generation task. The strong generalization potential of DT has inspired its application in various settings, including offline-to-online RL (Zheng et al., 2022) and meta-RL (Xu et al., 2022; Yang & Xu, 2025). However, to the best of our knowledge, no prior work has explicitly explored the adaptation capabilities of DT within the off-dynamics RL framework.

3 Preliminary

Sequential Decision-Making. We consider a general sequential decision-making problem. At each step t, the agent receives an observation o_t from the environment. Based on the history up to step t, the agent makes action a_t and receives the reward r_t from the environment. The agent interacts with the environment in episodes with a length H. We use $\tau = (o_1, a_1, r_1, \cdots, o_H, a_H, r_H)$ to denote a whole trajectory, and we use $g(\tau) = \sum_{t=1}^{H} r_t$ to denote the cumulative return of the trajectory τ. We model the environment as a Markov Decision Process (MDP) M, which consists of $(\mathcal{S}, \mathcal{A}, p, r, H)$. Here $\mathcal{S}$ is the state space, each state s represents the possible history up to some time step t, i.e., $s = (o_1, a_1, r_1, \cdots, o_t)$. $\mathcal{A}$ is the action space, $p(s'|s, a)$ is the transition dynamics that determines the transition probability for the agent to visit state s' from current state s with the action a. $r(s, a)$ denotes the reward function. We re-define a trajectory as $\tau = (s_1, a_1, r_1, \cdots, s_H, a_H, r_H)$. We assume that each s corresponds to one single time step $t = t(s)$, and we denote $g_\pi(s) = \mathbb{E}_{\tau \sim \pi}[g(\tau)|s_1 = s]$. Then the goal of the agent is to learn a policy $\pi : \mathcal{S} \to \mathcal{A}$ that maximizes the expected accumulated reward $J(\pi) := \mathbb{E}_{\tau \sim \pi}[g(\tau)]$. We denote the optimal policy as π^*.

Offline RL and Decision Transformer. We consider the offline reinforcement learning setting. Given a dataset $\mathcal{D}$, the goal of the agent is to learn π^* from $\mathcal{D}$. We assume that the trajectories in $\mathcal{D}$ are generated from a behavior policy β. In this work, we mainly consider Decision Transformer (DT) (Chen et al., 2021) as our backbone algorithm. DT is a type of sequential modeling technique based on Transformer (Vaswani et al., 2017) to solve offline RL problems. In detail, DT maintains a function $\pi(a|s, g)$ as its policy function. To train the policy π, DT aims to minimize the following negative log-likelihood function $\hat{L}(\pi) := \hat{L}(\pi) := -\sum_{\tau \in \mathcal{D}} \sum_{1 \leq t \leq H} \log \pi(a_t|s_t, g(\tau))$. To evaluate π, DT defines a *conditioning function* $f : \mathcal{S} \to \mathbb{R}$, which maps each state to a return value and guides the policy π_f within the environment, where $\pi_f(a|s) := \pi(a|s, f(s))$. The conditioning function is pivotal in DT, as varying $f(s)$ for a given state s results in different policies. To achieve the optimal policy, $f(s)$ should be maximized (Zhuang et al., 2024).

Offline Off-Dynamics RL. In this work, we consider the offline off-dynamics RL problem, where the agent has access to two offline datasets $\mathcal{D}^S$ and $\mathcal{D}^T$. $\mathcal{D}^S, \mathcal{D}^T$ include the data collected from the *source environment* M^S and the *target environment* M^T. The source and the target environments share the same reward function r, with different transition dynamics P^S and P^T. In practice, we assume that the dataset size from the source dataset $|\mathcal{D}^S|$ is much larger than the data coming from the target dataset $|\mathcal{D}^T|$. Then the agent aims to find the optimal policy for the target environment M^T based on the data from both the source and the target environments. Since the transition dynamics P^S and P^T are different, we can not directly apply existing RL algorithms on the union $\mathcal{D}^S \cup \mathcal{D}^T$.

4 Return Augmentation for Goal Conditioned Supervised Learning

4.1 Return-Augmented Framework

DT has the potential to address offline off-dynamics reinforcement learning challenges, as shown in Table 1. However, it still has certain limitations. To overcome these, we propose a general framework that efficiently learns the optimal policy for the target environment using the combined dataset $\mathcal{D}^S \cup \mathcal{D}^T$. Leveraging the return-conditioning nature of DT, we introduce a *return augmentation* technique that modifies returns in the offline source dataset through a transformation function. This approach allows the policy derived from the augmented source dataset to effectively approximate the optimal policy of the target environment, as illustrated in the following equation, where π^S represents a strong candidate for approximating the optimal policy of the target environment and ψ is the carefully chosen transformation function.

$$\pi^S = \arg\min_\pi \hat{L}(\pi) := -\sum_{\tau \in \mathcal{D}^S} \sum_{1 \leq t \leq H} \log \pi(a_t|s_t, \psi(g(\tau))).$$

We call our method *Return Augmented DT (REAG)*. Next we introduce two methods to construct ψ, based on the dynamics-aware reward augmentation (DARA) technique (Eysenbach et al., 2020; Liu et al., 2022), and a direct return distribution matching method.

4.2 Dynamics-Aware Reward Augmentation

We first summarize the idea of dynamics-aware reward augmentation (DARA) (Eysenbach et al., 2020; Liu et al., 2022). Let $P^T(s'|s, a)$ denote the transition dynamics of the target environment, and $p^S(s'|s, a)$ denote the source environment. According to the connection of RL and probabilistic inference (Levine, 2018), we can turn the optimal policy finding problem into an inference problem. We use O to denote a binary random variable where $O = 1$ suggests τ is a trajectory induced by the optimal policy. Given a trajectory τ, the likelihood of τ being a trajectory induced by the optimal policy under the target environment is $P^T(O = 1|\tau) = \exp(\sum_{t=1}^{H} r(s_t, a_t)/\eta)$, where η is the step size parameter used for tuning. It means that the trajectory with higher cumulative rewards is more likely to be the trajectory induced by the optimal policy. We introduce a variational distribution $P_\pi^S(\tau) = P(s_1) \prod_{t=1}^{T} P^S(s_{t+1}|s_t, a_t)\pi(a_t|s_t)$ to approximate $P_\pi^T(O = 1|\tau)$. Then we have

$$
\begin{aligned}
\log P_\pi^T(O = 1) &= \log \mathbb{E}_{\tau \sim P_\pi^T(\tau)} P^T(O = 1|\tau) \\
&\geq \mathbb{E}_{\tau \sim P_\pi^S(\tau)} \left[\log P^T(O = 1|\tau) + \log \left(P_\pi^T(\tau)/P_\pi^S(\tau) \right) \right] \\
&= \mathbb{E}_{\tau \sim P_\pi^S(\tau)} \left[\sum_{t=1}^{T} r(s_t, a_t)/\eta - \log \left(P^S(s_{t+1}|s_t, a_t)/P^T(s_{t+1}|s_t, a_t) \right) \right],
\end{aligned}
\tag{4.1}
$$

where for the first inequality, we change the distribution of the expectation from $P_\pi^T(\tau)$ to $P_\pi^S(\tau)$ and then use Jensen's inequality to derive the result; the second equation holds due to the assumption/modeling that the likelihood of τ being a trajectory induced by the optimal policy under the target environment is $P^T(O = 1|\tau) = \exp(\sum_{t=1}^H r(s_t, a_t)/\eta)$. Therefore, we obtain an evidence lower bound of $P_\pi^T(O = 1)$, which equals to find a policy to maximize the value in the source environment, with the augmented reward $r^S(s_t, a_t) = r(s_t, a_t) + \eta \log P^T(s_{t+1}|s_t, a_t) - \eta \log P^S(s_{t+1}|s_t, a_t)$. Following Eysenbach et al. (2020), to estimate the $\log P^T(s_{t+1}|s_t, a_t) - \log P^S(s_{t+1}|s_t, a_t)$, we use a pair of learned binary classifiers which infers whether the transitions come from the source or target environments. Specifically, we denote classifiers $q_{sas}(\cdot|s, a, s')$ and $q_{sa}(\cdot|s, a)$, which return the probability for some (s, a, s') or (s, a) tuples whether they belong to the source or the target environments. Then according to Eysenbach et al. (2020), we have

$$
\log P^T(s_{t+1}|s_t, a_t) - \log P^S(s_{t+1}|s_t, a_t) = \Delta r(s_t, a_t, s_{t+1})
$$
$$
:= \log \frac{q(M^T|s_t, a_t, s_{t+1})}{q(M^S|s_t, a_t, s_{t+1})} - \log \frac{q_{sa}(M^T|s_t, a_t)}{q_{sa}(M^S|s_t, a_t)}. \tag{4.2}
$$

For a trajectory $\tau = (s_1, a_1, r_1, ..., s_H, a_H, r_H)$, we denote the transformation $\psi(g(s_t)) := \sum_{h=t}^H r_h + \eta \sum_{h=t}^H \Delta r(s_h, a_h, s_{h+1})$. We denote such a transformation method as $\text{REAG}_{\text{Dara}}^*$.

4.3 Direct Matching of Return Distributions

The reward augmentation strategy in $\text{REAG}_{\text{Dara}}^*$ stems from the probabilistic inference view of RL which matches the distribution of the learning trajectory in the source domain with that of the optimal trajectory in the target domain (Eysenbach et al., 2020). However, it does not fully capture the power of DT, which is able to induce a *family of policies* that are conditioned on the return-to-go f. By varying f, DT enables the generation of a diverse range of policies, including the optimal one. In contrast, $\text{REAG}_{\text{Dara}}^*$ assumes a single, fixed target policy, and thus its augmentation strategy cannot generalize across multiple policies induced by varying f in DT. As a result, it cannot find the desired return conditioned policy when evaluated with a different f in the target domain. This motivates us to find a return transformation method ψ to guarantee that $\pi_f^S(a|s) \approx \pi_f^T(a|s)$ for all f.

We consider a simplified case where both D^S and D^T are generated by following the same behavior policy $\beta(a|s)$. We use $d_S(A)$ and $d_T(A)$ to denote the probability for event A to happen under the source and target environments following β. With a slight abuse of notation, we use g_S and g_T to denote the return following the behavior policy. Denote $g_S(s)$ and $g_T(s)$ ($g_S(s, a)$ and $g_T(s, a)$, resp.) as the random variables representing the return-to-go starting from s ((s, a), resp.) in the source and target domain. Then we characterize the learned policies by DT under the infinite data regime (Brandfonbrener et al., 2022) for both the source environment and target environment. According to Brandfonbrener et al. (2022), $\pi_f^S(a|s) = P^S(a|s, \psi(g_S) = f(s))$. Then we can express π^S and π^T as

$$
\pi_f^S(a|s) = \frac{d_S(a|s)d_S(\psi(g_S) = f(s)|s, a)}{d_S(\psi(g_S) = f(s)|s)}, \quad \pi_f^T(a|s) = \frac{d_T(a|s)d_T(g_T = f(s)|s, a)}{d_T(g_T = f(s)|s)}.
$$

Since the behavior policies over the source and target environments are the same, we have $d_S(a|s) = d_T(a|s)$ for all (s, a). Then in order to guarantee $\pi_f^S(a|s) = \pi_f^T(a|s)$ we only need to guarantee $d_S(\psi(g_S(s, a)) = \cdot|s, a) = d_T(g_T(s, a) = \cdot|s, a)$, $\forall s, a$. Denote the cumulative distribution function (CDF) of g_S conditioned on s, a is $g_S|s, a \sim G_\beta^S(s, a)$, and $g_T|s, a \sim G_\beta^T(s, a)$. Then if both $G_\beta^S(s, a)$ and $G_\beta^T(s, a)$ are invertible, we can set ψ as follows

$$
\psi(g_S) = G_\beta^{T,-1}(G_\beta^S(g_S; s, a); s, a). \tag{4.3}
$$

If there exist P^S, P^T, and r such that the DARA-type augmented reward-to-go satisfies (4.3), then the DARA-type reward augmentation can be deemed as a special case of the transformation (4.3). In general, G_β^T and G_β^S are hard to obtain and computationally intractable, making ψ intractable either. We use Laplace approximation to approximate both G_β^T and G_β^S by Gaussian distributions, e.g., $G_\beta^S(s, a) \sim N(\mu^S(s, a), \sigma_S^2(s, a))$

and $G_\beta^T(s,a) \sim N(\mu^T(s,a), \sigma_T^2(s,a))$. Then it is easy to obtain that

$$\psi(g_S) := \frac{g_S - \mu^S(s,a)}{\sigma^S(s,a)} \cdot \sigma^T(s,a) + \mu^T(s,a). \tag{4.4}$$

We denote DT with a ψ transformation from (4.4) by $\text{REAG}_{\text{MV}}^*$, since such a transformation only depends on the estimation of mean values μ^S, μ^T and variance σ^S, σ^T.

4.4 Sample Complexity of Off-Dynamics RCSL

In this section, we provide finite sample analysis of the sample complexity of the off-dynamics RCSL. To this end, we first define some useful notations. We assume there are N^S trajectories in the source dataset $\mathcal{D}^S$, and N^T trajectories in the target dataset $\mathcal{D}^T$. Denote P_β^S as the joint distribution of state, action, reward and return-to-go induced by the behavior policy β in the source environment, and P_β^T in the target environment. Denote d_π^S as the marginal distribution of state s induced by any policy π in the source environment, and d_π^T in the target environment.

Denote $J^T(\pi)$ as the expected cumulative reward under any policy π and the target environment. For any return-to-go g in the source dataset $\mathcal{D}^S$, we transform g by an oracle defined in (4.3) with others remain the same, then we get a modified dataset $\tilde{D}^S$. We denote the mixed dataset as $\mathcal{D} = \mathcal{D}^T \cup \tilde{\mathcal{D}}^S$. Our theorem is established based on the following assumptions.

Assumption 4.1. (1) (Near determinism) $P^T(r \neq r(s,a) \text{ or } s' \neq \xi(s,a)|s,a) \leq \epsilon$ at all s,a for some functions ξ and r. (2) (Consistency of f) $f(s) = f(s') + r$ for all s.

Assumption 4.2. For all s we assume (1) (Bounded occupancy mismatch) $P_{\pi_f^{\text{RCSL}}}^T(s) \leq C_f P_\beta^T(s)$; (2) (Return coverage) $P_\beta^T(g = f(s)|s) \geq \alpha_f$; and (3) (Domain occupancy overlap) $d_\beta^T(s) \leq \gamma_f d_\beta^S(s)$.

Assumption 4.3. (1) The policy class Π is finite. (2)$|\log \pi(a|s,g) - \log \pi(a'|s',g')| \leq c$ for any (a,s,g,a',s',g') and all $\pi \in \Pi$. (3) The approximation error is bounded by ϵ_{approx}, i.e., $\min_{\pi \in \Pi} L(\pi) \leq \epsilon_{\text{approx}}$.

Assumptions 4.1 to 4.3 are the same as the assumptions imposed in Theorem 1, Theorem 2, and Corollary 3 in Brandfonbrener et al. (2022) respectively.

We first show the sample complexity of DT with only the samples from the target dataset $\mathcal{D}^T$. If we only use the offline dataset $\mathcal{D}^T$ collect from the target environment, i.e., at training time we minimizes the empirical negative log-likelihood loss:

$$\hat{L}^T(\pi) = - \sum_{\tau \in \mathcal{D}^T} \sum_{1 \leq t \leq H} \log \pi(a_t|s_t, g(s_t)).$$

Then we get the following sample complexity guarantee based on the result in Brandfonbrener et al. (2022).

Corollary 4.4. There exists a conditioning function $f : \mathcal{S} \to \mathbb{R}$ such that assumptions (1) and (2) in Assumption 4.1, and (1) and (2) in Assumption 4.2 hold. Further suppose Assumption 4.3 holds. Then for some $\delta \in (0,1)$, with probability at least $1 - \delta$, we have

$$J^T(\pi^\star) - J^T(\hat{\pi}_f) \leq O\left(\frac{C_f}{\alpha_f} H^2 \left(\sqrt{c}\left(\frac{\log |\Pi|/\delta}{N^T}\right)^{1/4} + \sqrt{\epsilon_{\text{approx}}}\right) + \frac{\epsilon}{\alpha_f} H^2\right).$$

Now we consider the case of mixed dataset, where we train our policy on both the target dataset and the source dataset using the proposed returned conditioned decision transformer methods. Note that the size of the target environment dataset is usually small, while the size of the source environment dataset is much larger, that is, $N^T \ll N^S$. If we incorporate the modified source dataset into the supervised learning, that is, we minimize the following empirical negative log-likelihood loss:

$$\hat{L}^{\text{mix}}(\pi) = - \sum_{\tau \in \mathcal{D}} \sum_{1 \leq t \leq H} \log \pi(a_t|s_t, g(s_t)). \tag{4.5}$$

An observation is that, with the modified source dataset, the regret $J^T(\pi^\star) - J^T(\hat{\pi}_f)$ can be significantly reduced. This is formulated in the following theorem.

Theorem 4.5. There exists a conditioning function f such that Assumptions 4.1 and 4.2 hold. Further assume Assumption 4.3 holds. Then for some $\delta \in (0, 1)$, with probability at least $1 - \delta$, we have

$$J^T(\pi^\star) - J^T(\hat{\pi}_f) \leq O\Big(\frac{C_f}{\alpha_f} \cdot \frac{N^S + N^T}{N^S/\gamma_f + N^T} \cdot H^2 \cdot \Big(\sqrt{c}\Big(\frac{\log|\Pi|/\delta}{N^T + N^S}\Big)^{1/4} + \sqrt{\epsilon_{\text{approx}}}\Big) + \frac{\epsilon}{\alpha_f} \cdot H^2\Big). \qquad (4.6)$$

Remark 4.6. Compared to Corollary 4.4, Theorem 4.5 suggests that the modified samples from the source domain could enhance the performance of RCSL when the domain occupancy overlap coefficient γ_f is large. In particular, when $N^S \gg N^T$ and $\gamma_f = O(1)$, (4.6) can be simplified to

$$J^T(\pi^\star) - J^T(\hat{\pi}_f) \leq O\Big(\frac{C_f}{\alpha_f} H^2 \Big(\sqrt{c}\Big(\frac{\log|\Pi|/\delta}{N^S}\Big)^{1/4} + \sqrt{\epsilon_{\text{approx}}}\Big) + \frac{\epsilon}{\alpha_f} H^2\Big),$$

which significantly improves the bound on suboptimality in Corollary 4.4.

5 Experiments

In this section, we first outline the fundamental setup of the experiment. We then describe experiments designed to address specific questions, with each question and its corresponding answer detailed in a separate subsection.

- How effective are DT-type methods in mitigating the impact of offline data shortages in target environment?
- What techniques can be employed to improve the performance of DT-type methods in off-dynamics scenarios while addressing the constraints of offline data shortages in target environment?
- How does the performance of DT-type methods compare to other approaches in solving off-dynamics problems?

5.1 Basic Experiment Setting

Tasks and Environments. We study established D4RL tasks in the Gym-MuJoCo environment (Fu et al., 2020), a suite built atop the MuJoCo physics simulator, featuring tasks such as locomotion and manipulation. Particularly, we focused on three environments: Walker2D, Hopper, and HalfCheetah. In addressing the off-dynamics reinforcement learning problem, we distinguish between the Source and Target environments. The Target environment is based on the original Gym-MuJoCo framework, while the Source environment is modified using two shift methods: BodyMass Shift and JointNoise Shift. In the BodyMass Shift, the mass of the body is altered in the Source environment, whereas in the JointNoise Shift, random noise is added to the actions.

Dataset. For the Target Dataset corresponding to the Target Environment, we leverage the official D4RL data to construct the target datasets: 10T and 1T. The 10T dataset comprises ten times the number of trajectories compared to the 1T dataset.[1] For the Source Dataset collection, we begin by modifying the environment through adjustments to the XML file of the MuJoCo simulator. We then collect the Random, Medium, Medium-Replay, and Medium-Expert offline datasets in the modified environments, following the same data collection procedure as used in D4RL. For further details on the dataset collection process and the datasets, please refer to the Appendix B.

Baselines. We consider a diverse set of established off-dynamics RL methods as baselines, including BEAR (Kumar et al., 2019), AWR (Peng et al., 2019), BCQ (Fujimoto et al., 2019), CQL (Kumar et al., 2020), and MOPO (Yu et al., 2020). We further include their DARA-augmented variants (Liu et al., 2022) as additional baselines for comparison. In addition, we evaluate recent dynamics-aware methods, including

---

[1]Unlike the approach of Liu et al. (2022), which constructs the 1T dataset by selecting the last 1/10 timesteps from the original target dataset (10T), we propose a uniform sampling method across trajectories in the target dataset.

	BEAR			AWR			BCQ			CQL		
	M	M-R	M-E	M	M-R	M-E	M	M-R	M-E	M	M-R	M-E
1T	$4.638_{\pm3.882}$	$0.777_{\pm0.105}$	$9.267_{\pm1.692}$	$68.023_{\pm1.687}$	$28.426_{\pm2.974}$	$100.566_{\pm0.513}$	$62.567_{\pm2.459}$	$60.638_{\pm0.683}$	$101.610_{\pm1.309}$	$65.618_{\pm2.818}$	$57.402_{\pm6.161}$	$101.611_{\pm0.143}$
10T	$13.143_{\pm3.016}$	$5.852_{\pm0.168}$	$21.383_{\pm1.237}$	$78.060_{\pm0.772}$	$58.286_{\pm1.684}$	$109.154_{\pm0.976}$	$74.735_{\pm1.184}$	$64.735_{\pm2.555}$	$101.840_{\pm1.962}$	$78.191_{\pm1.839}$	$80.145_{\pm2.286}$	$101.840_{\pm0.467}$
	MOPO			DT			Reinformer			QT		
	M	M-R	M-E	M	M-R	M-E	M	M-R	M-E	M	M-R	M-E
1T	$20.953_{\pm2.715}$	$20.313_{\pm3.488}$	$20.569_{\pm0.983}$	$67.261_{\pm2.316}$	$34.482_{\pm5.890}$	$107.171_{\pm1.611}$	$79.034_{\pm1.506}$	$38.072_{\pm9.174}$	$103.284_{\pm5.437}$	$81.756_{\pm1.671}$	$67.546_{\pm9.505}$	$111.722_{\pm1.398}$
10T	$22.261_{\pm2.811}$	$18.529_{\pm1.760}$	$21.196_{\pm3.103}$	$79.697_{\pm3.348}$	$68.528_{\pm1.924}$	$108.622_{\pm1.815}$	$81.377_{\pm1.903}$	$68.168_{\pm2.661}$	$109.845_{\pm0.726}$	$88.262_{\pm12.886}$	$85.092_{\pm8.727}$	$111.394_{\pm0.469}$

Table 1: Performance comparison of algorithms on the **1T**, **10T**, and **1T10S** datasets. In this study, **1T10S(B)** refers to the source dataset under the **BodyMass shift** setting, while **1T10S(J)** corresponds to the source dataset under the **JointNoise shift** setting. Experiments are conducted using the **Medium (M)**, **Medium-Replay (M-R)**, and **Medium-Expert (M-E)** datasets. We present the results for the **Walker2D** environment here; complete results are provided in Appendix C.1. All reported values are averaged over five seeds (0, 1012, 2024, 3036, 4048).

DFDT (Wang et al., 2025), H2O (Niu et al., 2022), and IGDF (Wen et al., 2024).For hyperparameter selection, we use consistent settings across tasks for shared parameters, such as the learning rate and the number of training iterations. Detailed configurations are provided in Appendix B. parameter settings.

5.2 Evaluation of Adaptability and Data Efficiency in RCSL Algorithms

We evaluate three representative DT-type algorithms include DT (Chen et al., 2021), QT (Hu et al., 2024), and Reinformer (Zhuang et al., 2024) to assess their ability to enable an adaptive policy while reducing reliance on offline data in the target environment. To conduct this evaluation, we perform two experiments: (1) We examine the performance of the three DT-type algorithms under varying dataset sizes and quality levels in the target environment; (2) We evaluate their effectiveness in off-dynamics scenarios.

To assess the impact of dataset size and quality on the performance of DT-type algorithms, we evaluate three algorithms using two datasets: a subset of the target data (1T) and the full target dataset (10T), comparing the results against other baselines. These experiments aim to quantify the performance gap between training on 1T and 10T datasets, highlighting the effects of target environment data scarcity and establishing a benchmark for off-dynamics settings. In off-dynamics offline RL, instead of relying solely on a large target dataset, we incorporate a small subset of target data with a larger source dataset. To examine how effectively algorithms leverage source data, we construct the 1T10S dataset by combining a subset of target data (1T) with the full source dataset (10S), following the setting of Liu et al. (2022). This dataset serves as the training set for DT-type algorithms, whose performance is then evaluated in the target environment. For a comprehensive comparison, we benchmark DT-type algorithms against other baseline methods.

Table 1 presents the evaluation results, illustrating the impact of dataset size and off-dynamics settings on algorithm performance. Limited training data constrains the algorithm's learning capacity, leading to degraded performance, particularly when the target environment data is scarce. To mitigate this issue, additional source datasets are incorporated under BodyMass Shift and JointNoise Shift settings, improving generalization to the target environment. While leveraging source data can partially compensate for the lack of target data, it remains suboptimal compared to training with sufficient target environment data. To enhance the effectiveness of DT-type frameworks in off-dynamics settings, we propose two return-based augmentation methods: $\text{REAG}^*_{\text{MV}}$ and $\text{REAG}^*_{\text{Dara}}$, which can be applied to DT, Reinformer, and QT frameworks. Specifically, applying $\text{REAG}^*_{\text{MV}}$ results in **$\text{REAG}^{\text{DT}}_{\text{MV}}$**, **$\text{REAG}^{\text{Reinf}}_{\text{MV}}$**, and **$\text{REAG}^{\text{QT}}_{\text{MV}}$**, while applying $\text{REAG}^*_{\text{Dara}}$ leads to **$\text{REAG}^{\text{DT}}_{\text{Dara}}$**, **$\text{REAG}^{\text{Reinf}}_{\text{Dara}}$**, and **$\text{REAG}^{\text{QT}}_{\text{Dara}}$**, demonstrating the potential of these augmentation techniques in improving algorithm performance under off-dynamics setting.

5.3 Return Augmentation Methods for Off-Dynamics RL

Here we discuss how to implement $\text{REAG}^*_{\text{MV}}$ and $\text{REAG}^*_{\text{Dara}}$ in practice. We implement $\text{REAG}^*_{\text{Dara}}$ based on the dynamics-aware reward augmentation method proposed in Liu et al. (2022). For $\text{REAG}^*_{\text{MV}}$, it involves training the CQL model across both the Target and Source Environments to derive the respective value

			DT			Reinformer			QT		
			1T10S	REAG$_{\text{MV}}^{\text{DT}}$	REAG$_{\text{Dara}}^{\text{DT}}$	1T10S	REAG$_{\text{MV}}^{\text{Reinf}}$	REAG$_{\text{Dara}}^{\text{Reinf}}$	1T10S	REAG$_{\text{MV}}^{\text{QT}}$	REAG$_{\text{Dara}}^{\text{QT}}$
W2D	M	BM	78.768±1.233	80.857±1.715↑	78.257±2.423↓	80.857±0.509	82.354±1.479↑	80.666±0.505↓	84.325±0.425	84.582±0.507↑	83.068±0.859↓
		JN	71.068±1.022	75.008±1.834↑	71.779±1.706↑	74.748±1.721	75.008±0.986↑	74.268±1.341↓	80.621±1.143	80.904±1.502↑	78.672±2.201↓
	M-R	BM	73.664±1.920	73.708±1.570↑	67.565±0.799↓	67.032±5.767	50.296±14.211↓	66.658±4.303↑	87.292±0.631	87.491±1.226↑	76.169±7.567↓
		JN	58.255±3.181	55.722±2.653↓	62.226±0.383↑	54.801±3.217	47.591±10.244↓	55.438±4.833↑	82.139±1.029	82.363±4.206↑	79.795±4.708↓
	M-E	BM	84.430±0.823	88.235±1.886↑	85.328±0.865↑	83.388±0.806	84.897±1.117↑	83.761±0.735↓	93.082±0.348	92.744±0.499↓	94.578±1.383↑
		JN	115.746±1.116	111.060±2.247↓	111.236±0.914↓	117.360±2.550	118.218±1.460↑	117.765±2.499↑	116.149±1.640	118.564±0.697↑	116.115±1.889↓
Hp	M	BM	34.057±0.177	39.435±1.239↑	37.787±1.914↑	51.357±3.713	59.085±2.791↑	51.771±5.322↑	49.516±9.798	51.796±9.971↑	62.262±5.348↑
		JN	70.685±0.726	70.356±3.657↓	78.325±2.522↑	70.340±4.633	72.346±5.877↑	70.466±3.728↑	68.656±7.079	73.987±8.080↑	68.709±12.160↑
	M-R	BM	64.216±1.504	66.092±0.233↑	60.393±1.086↓	17.534±6.725	20.952±9.794↑	27.238±12.735↑	69.460±13.948	76.287±7.810↑	82.786±11.992↑
		JN	61.870±0.249	77.825±1.638↑	83.525±1.728↑	41.820±15.773	43.985±5.075↑	52.052±10.035↑	93.704±7.559	93.409±4.696↓	51.456±12.168↓
	M-E	BM	33.554±0.846	52.873±0.454↑	33.631±1.605↑	68.973±7.512	64.206±12.073↓	73.363±7.674↑	61.162±3.767	73.952±16.294↑	77.279±18.607↑
		JN	108.254±1.583	109.367±1.084↑	108.261±2.612↑	109.256±0.126	109.472±0.103↑	109.255±0.188↓	109.056±0.214	109.803±0.609↑	109.746±0.771↑
Hc	M	BM	39.954±0.260	40.250±0.911↑	37.599±0.395↓	37.353±0.483	42.451±0.491↑	38.261±1.238↑	44.656±0.643	47.303±0.318↑	46.383±0.358↑
		JN	47.725±0.431	44.149±3.672↓	47.833±0.284↑	48.274±0.191	43.009±0.307↓	48.404±0.168↑	56.213±0.327	52.394±1.413↓	55.026±0.410↓
	M-R	BM	20.966±9.607	27.812±3.256↑	24.059±2.271↑	31.584±1.248	32.114±1.455↑	26.995±4.373	41.300±0.787	42.405±0.729↑	41.359±0.985↑
		JN	36.509±4.414	38.417±4.068↑	38.031±3.529↑	40.296±2.914	40.840±2.880↑	38.436±3.377↓	53.763±0.793	53.870±0.981↑	53.257±0.586↓
	M-E	BM	54.981±1.147	56.228±2.930↑	51.357±8.231↓	40.568±0.984	46.048±1.657↑	55.818±1.849↑	71.080±8.802	69.819±5.120↓	76.533±8.022↑
		JN	70.573±8.599	77.762±2.099↑	77.751±2.702↑	76.073±3.878	79.390±0.149↑	78.981±1.198↑	82.961±4.019	83.692±0.699↑	82.148±2.758↓

Table 2: Performance evaluation of two return augmentation methods, **REAG$_{\text{MV}}^{*}$** and **REAG$_{\text{Dara}}^{*}$**, integrated with **DT**, **Reinformer**, and **QT** frameworks in off-dynamics scenarios. The experiments are conducted in the **Walker2D (W2D)**, **Hopper (Hp)**, and **HalfCheetah (Hc)** environments under the **Medium (M)**, **Medium-Replay (M-R)**, and **Medium-Expert (M-E)** settings. The source environment is modified using two shift conditions: **BodyMass shift (BM)** and **JointNoise shift (JN)**. For reference, the table also includes the performance of the original DT-type methods without augmentation, displayed in gray font. Performance changes due to augmentation are indicated with red upward arrows (↑) for improvements and green downward arrows (↓) for degradations compared to the original DT-type methods. All reported values are averaged over five random seeds (0, 1012, 2024, 3036, 4048).

functions, denoted as Q_T and Q_S. The derived value functions are then used to relabel the returns of trajectories in the original dataset. More specifically, the relabeled return $\hat{g}^S$ is calculated as defined in (4.4). Within this framework, we use $\mu^S(s,a)$ to denote $Q_S(s,a)$, and $Q_T(s,a)$ corresponds to $\mu^T(s,a)$. For the computation of $\sigma_S(s,a)$ and $\sigma_T(s,a)$, we employ the following methodology: For a given state s, we use the policy of CQL on the source dataset to obtain n available actions $\{a_1^S, a_2^S, \ldots, a_n^S\}$ given the state s, with the corresponding Q values $\{Q_S(s,a_1^S), Q_S(s,a_2^S), \ldots, Q_S(s,a_n^S)\}$, and n available actions $\{a_1^T, a_2^T, \ldots, a_n^T\}$ in the target environment obtained from the CQL policy trained over the target dataset, with the corresponding Q values $\{Q_T(s,a_1^T), Q_T(s,a_2^T), \ldots, Q_T(s,a_{n'}^T)\}$. The standard deviations $\sigma_S(s,a)$ and $\sigma_T(s,a)$ are then calculated as specified as follows.

$$\sigma_S(s,a) = \text{std}(Q_S(s,a_1^S), Q_S(s,a_2^S), \ldots, Q_S(s,a_n^S)),$$
$$\sigma_T(s,a) = \text{std}(Q_T(s,a_1^T), Q_T(s,a_2^T), \ldots, Q_T(s,a_n^T)).$$

For a detailed discussion, please refer to Section 4. As defined in (4.4), computing the ratio $\frac{\sigma_T(s,a)}{\sigma_S(s,a)}$ is essential. However, extreme values of this ratio can lead to instability during training. To address this, we introduce a clipping technique that constrains the ratio within an upper bound θ_1 and a lower bound θ_2. This helps stabilize REAG$_{\text{MV}}^{*}$ training by mitigating two key challenges. First, since this ratio depends on the variance of return-to-go in both the source and target environments, extreme variance values can introduce large gradients or noisy updates, destabilizing training. Second, variance is estimated using the Q-value function learned through CQL on the source and target datasets, which may introduce estimation errors. By bounding the ratio within a controlled range, clipping reduces the impact of these errors and prevents instability.

Table 2 presents a performance comparison of the REAG$_{\text{MV}}^{*}$ and REAG$_{\text{Dara}}^{*}$ return augmentation techniques integrated into different DT-type frameworks, including DT, Reinformer, and QT, in off-dynamics scenarios. Evaluations are conducted across three Gym environments—Walker2D, Hopper, and HalfCheetah—under three dataset settings: Medium, Medium-Replay, and Medium-Expert. To simulate off-dynamics conditions, two domain shifts, BodyMass Shift and JointNoise Shift, are introduced. The results demonstrate that
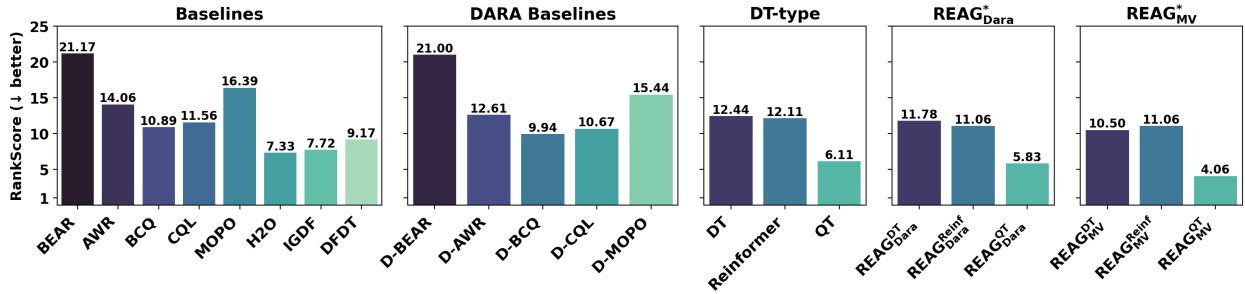
Figure 1: Average normalized rank scores for all baseline algorithms across the Medium, Medium-Replay, and Medium-Expert datasets under BodyMass and JointNoise shift settings in the Walker2D, Hopper, and HalfCheetah environments. Within each setting, algorithms were ranked based on performance, with the top-performing algorithm assigned a rank of 1. Tied scores received the same rank, with subsequent ranks adjusted accordingly. Lower rank scores indicate better overall performance. The original ranks (from 22 algorithms) were normalized to a scale of 1 to 22. The figure presents the average normalized rank scores across the Walker2D, Hopper, and HalfCheetah environments.
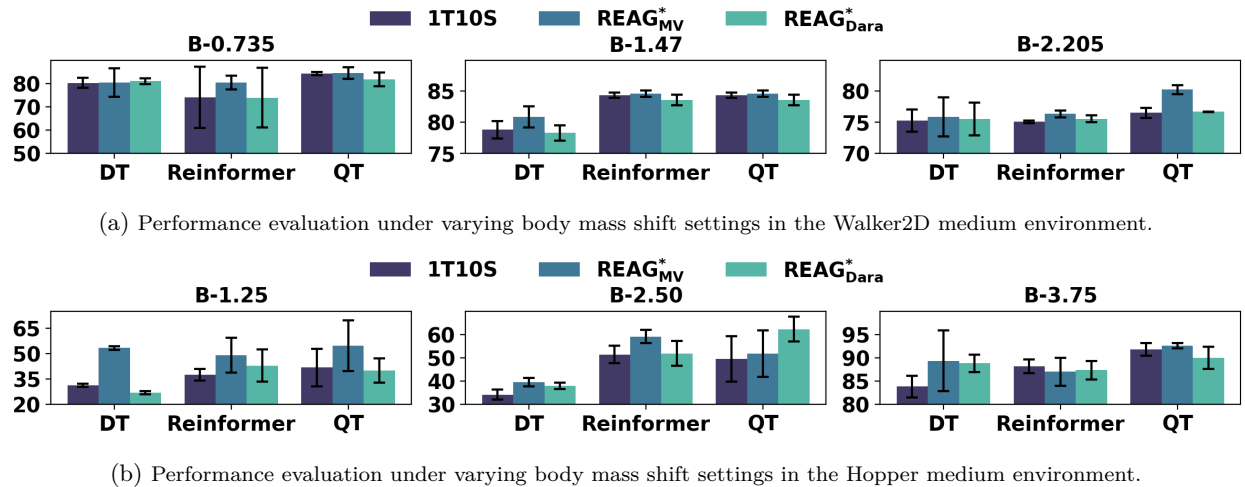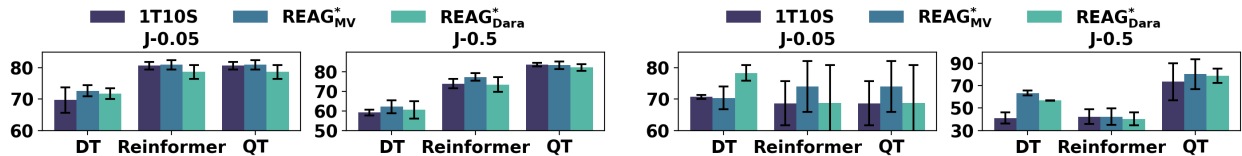

(a) Performance evaluation under varying body mass shift settings in the Walker2D medium environment.

(b) Performance evaluation under varying body mass shift settings in the Hopper medium environment.

Figure 2: Performance of $\mathbf{REAG^*_{MV}}$ and $\mathbf{REAG^*_{Dara}}$ algorithms under different body mass shift settings in the Walker2D and Hopper medium environments. **"B-x"** denotes that the body mass in the simulator is set to **x**. The target body mass is **2.94** in the Walker2D environment and **5** in the Hopper environment.

both $\text{REAG}^*_{\text{MV}}$ and $\text{REAG}^*_{\text{Dara}}$ effectively enhance DT-type frameworks, improving performance in most off-dynamics scenarios compared to their original, non-augmented counterparts. Specifically, $\text{REAG}^*_{\text{MV}}$, which augments based on return values, leverages information from both the source and target environments, making it particularly well-suited for return-based algorithms. In contrast, $\text{REAG}^*_{\text{Dara}}$, which augments based on reward values, exhibits more variable performance across different environments and dataset settings. While $\text{REAG}^*_{\text{Dara}}$ improves performance in certain cases, $\text{REAG}^*_{\text{MV}}$ delivers more stable and robust improvements in the most cases. DARA is a widely adopted approach for addressing off-dynamics RL problems by introducing reward augmentation to enhance policy adaptation from a source dataset to a target environment while minimizing reliance on extensive target data. It seamlessly integrates with traditional offline RL frameworks such as CQL and BCQ. In our evaluation, we compare our proposed methods against DARA-based approaches, including both traditional RL frameworks and their DARA-augmented variants, as well as DT-type frameworks with and without $\text{REAG}^*_{\text{MV}}$ and $\text{REAG}^*_{\text{Dara}}$ augmentation, providing a comprehensive assessment of augmentation techniques for off-dynamics adaptation. We present a comparative ranking where lower average rank scores indicate better overall performance, as shown in Figure 1; for the raw results of each setting, please refer to Appendix C.1. The results demonstrate that DT-type frameworks exhibit strong potential in solving off-dynamics RL problems, outperforming traditional offline RL methods, particularly in the case of QT. Return-based augmentation techniques further enhance effectiveness, with

(a) Performance evaluation under varying joint noise shift settings in the Walker2D medium environment.

(b) Performance evaluation under varying joint noise shift settings in the Hopper medium environment.

Figure 3: Performance of $\mathbf{REAG^*_{MV}}$ and $\mathbf{REAG^*_{Dara}}$ algorithms across varying JointNoise shift settings in the Walker2D and Hopper medium environments. **"J-x"** denotes the addition of random noise in the range **(-x, +x)** to the action.

$\text{REAG}^*_{\text{MV}}$ and $\text{REAG}^{\text{QT}}_{\text{MV}}$ achieving state-of-the-art performance compared to other baselines. Additionally, while DARA effectively improves the performance of non-return-based offline RL methods, a noticeable gap remains between these approaches and DT-type methods.

5.4 Ablation Studies for Return Augmentation Methods

In this section, we present an ablation study to identify the key factors affecting $\text{REAG}^*_{\text{Dara}}$ and $\text{REAG}^*_{\text{MV}}$ algorithm performance. We study the following variation settings.

- **(Dynamics Shift)** How do $\mathbf{REAG^*_{MV}}$ and $\mathbf{REAG^*_{Dara}}$ methods perform under significantly shifted source environments?
- **(Clipped Augmented Return)** What is the impact of the clipping technique in $\mathbf{REAG^*_{MV}}$ on its performance?
- **(Consistent Augmented Return)** How does consistency affect the performance of $\mathbf{REAG^*_{MV}}$?
- **(Return Learning)** How accurate is the estimation of the learned value function in $\mathbf{REAG^*_{MV}}$?

Dynamics Shift. To evaluate the impact of shifting source environments on $\text{REAG}^*_{\text{MV}}$ and $\text{REAG}^*_{\text{Dara}}$, we assess their performance under various BodyMass and JointNoise shift settings. The experimental results are presented in Figures 2 and 3. Our findings indicate that as the body mass shift increases—creating a greater discrepancy from the target environment—performance deteriorates in both the Walker2D and Hopper Medium environments. Similarly, introducing higher levels of action noise leads to a decline in performance, suggesting that increased random noise raises the likelihood of failure, ultimately resulting in poorer outcomes. This performance degradation is particularly evident in the DT framework, highlighting its sensitivity to off-dynamics shifts, whereas Reinformer and QT demonstrate greater robustness. Across all shift experiments, $\text{REAG}^*_{\text{MV}}$ consistently outperforms $\text{REAG}^*_{\text{Dara}}$, with the performance gap becoming especially pronounced under larger shifts, such as in the Hopper environment with a body mass shift of 1.25.

Clipped Augmented Return. For data augmentation in $\text{REAG}^*_{\text{MV}}$, we apply a clipping technique to prevent the occurrence of extreme values. To evaluate its impact, we compare the performance of $\text{REAG}^*_{\text{MV}}$ with and without clipping in the Walker2D, Hopper, and HalfCheetah Medium Expert environments under BodyMass shifts. The results, presented in Figure 4, demonstrate that mitigating extreme values generally enhances the performance of $\text{REAG}^*_{\text{MV}}$. Additionally, we observe that for $\text{REAG}^{\text{QT}}_{\text{MV}}$, clipping does not yield significant improvements compared to DT and Reinformer. We hypothesize that this is due to the QT mechanism, which inherently regularizes the return, whereas DT and Reinformer lack such a mechanism.

Consistent Augmented Return. It is worth noting that our augmented target returns do not satisfy the *consistency condition*, which requires that the augmented returns follow $R_{t+1} - R_t = r_t$, as enforced by the original DT. To verify whether consistency is a necessary condition for augmentation in off-dynamics settings, we conduct the following ablation study. Specifically, we introduce a variant of $\text{REAG}^*_{\text{MV}}$, denoted as $\text{REAG}^*_{\text{MV}}$ (consistent), where for each trajectory in the target environment, return augmentation is applied only to the initial return, while all subsequent augmented returns are derived using the consistency condition $R_{t+1} - R_t = r_t$. The results, presented in Figure 5, indicate that $\text{REAG}^*_{\text{MV}}$ outperforms its consistency-enforced variant in most cases. This finding suggests that enforcing consistency does not neces-
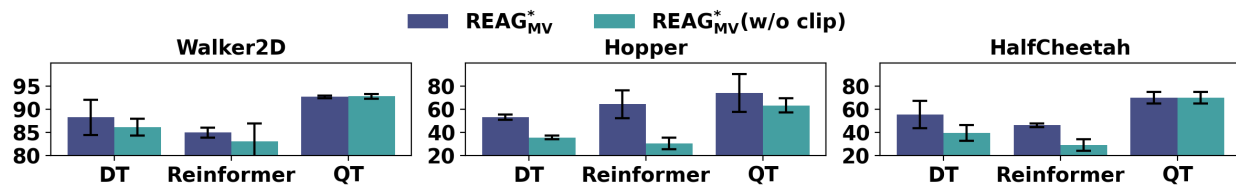
Figure 4: Comparison of $REAG^*_{MV}$ with and without the clipping technique in the Medium Expert setting of the Walker2D environment under BodyMass shift. Results are averaged over five seeds.
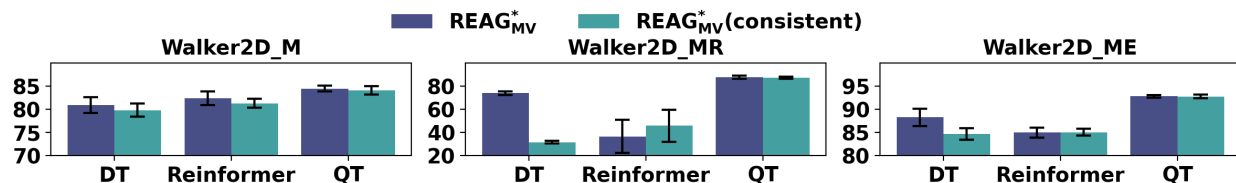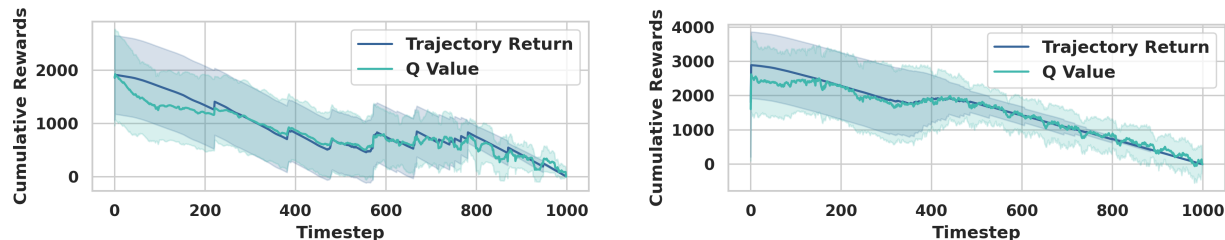

Figure 5: Comparison of $REAG^*_{MV}$ and $REAG^*_{MV}$(consistent) across Medium, Medium Replay, and Medium Expert settings in the Walker2D environment under BodyMass shift. Results are averaged over five seeds.

(a) Comparison between cumulative rewards and estimated Q_S values in the source environment with 100 trajectories.

(b) Comparison between cumulative rewards and estimated Q_T values in the target environment with 100 trajectories.

Figure 6: Comparison of the cumulative returns and the learned Q-values for the source (left) and target (right) environments using CQL. Results are plotted with the mean and variance of 100 trajectories.

sarily improve performance; instead, it may limit the effectiveness of $REAG^*_{MV}$ in the context of off-dynamics offline reinforcement learning.

Return Learning. To evaluate the learned value functions, Q_S and Q_T, and their impact on $REAG^*_{MV}$, we conduct an ablation experiment. Specifically, we assess the quality of the learned value functions in both the source and target domains. We select the Hopper environment with a medium-expert offline dataset as the target domain and the BodyMass shift as the source domain. Ideally, the value functions Q_S and Q_T learned through $REAG^*_{MV}$ should accurately reflect the returns of trajectories in their respective domains. To verify this, we train two additional DTs separately on the source and target offline datasets to obtain policies for these environments. Using these policies, we generate test trajectories through rollouts and then leverage the learned value functions Q_S and Q_T, trained on the 10S and 1T datasets, to predict the returns of these test trajectories. By comparing the predicted returns with the actual returns, we assess the accuracy of the learned value functions. As shown in Figure 6, our learned value functions Q_S and Q_T accurately reflect the returns of trajectories collected by the policies in the source and target environments, demonstrating that the Q-values used in our approach serve as reliable approximations.

6 Conclusion and Future Work

We introduced the Return Augmented (REAG) method for improving the performance of decision transformer type of methods in off-dynamics reinforcement learning which augments the return function of trajec-

tories from the source environment to better align with the target environment. We presented two practical implementations: $\text{REAG}^*_{\text{Dara}}$, derived from existing dynamic programming reward augmentation techniques, and $\text{REAG}^*_{\text{MV}}$, which matches the mean and variance of the return function under a Gaussian approximation of the return distribution. Through rigorous theoretical analysis, we showed that REAG when trained only on the source domain's dataset can achieve the same level of suboptimality as policies learned directly in the target domain. Our experiments demonstrate that REAG boosts various DT-type baseline algorithms in off-dynamics RL, and outperforms many dynamic programming based algorithms in this setting. This work establishes REAG as a promising method for leveraging source domain data to improve policy learning in target domains with limited data, thus addressing key challenges in offline, off-policy, and off-dynamics RL. Future work could explore extensions and applications of REAG in more diverse RL environments and further refine the augmentation techniques to enhance efficiency and effectiveness.

Acknowledgments

References

David Brandfonbrener, Alberto Bietti, Jacob Buckman, Romain Laroche, and Joan Bruna. When does return-conditioned supervised learning work for offline reinforcement learning? *Advances in Neural Information Processing Systems*, 35:1542–1553, 2022. 2, 3, 5, 6, 16, 23, 26

Lili Chen, Kevin Lu, Aravind Rajeswaran, Kimin Lee, Aditya Grover, Misha Laskin, Pieter Abbeel, Aravind Srinivas, and Igor Mordatch. Decision transformer: Reinforcement learning via sequence modeling. *Advances in neural information processing systems*, 34:15084–15097, 2021. 2, 3, 4, 8, 18

Scott Emmons, Benjamin Eysenbach, Ilya Kostrikov, and Sergey Levine. Rvs: What is essential for offline rl via supervised learning? *arXiv preprint arXiv:2112.10751*, 2021. 2, 3

Benjamin Eysenbach, Swapnil Asawa, Shreyas Chaudhari, Sergey Levine, and Ruslan Salakhutdinov. Off-dynamics reinforcement learning: Training for transfer with domain classifiers. *arXiv preprint arXiv:2006.13916*, 2020. 1, 2, 3, 4, 5

Justin Fu, Aviral Kumar, Ofir Nachum, George Tucker, and Sergey Levine. D4rl: Datasets for deep data-driven reinforcement learning. *arXiv preprint arXiv:2004.07219*, 2020. 7

Scott Fujimoto, David Meger, and Doina Precup. Off-policy deep reinforcement learning without exploration. In *International conference on machine learning*, pp. 2052–2062. PMLR, 2019. 7, 18

Haiyuan Gui, Shanchen Pang, Shihang Yu, Sibo Qiao, Yufeng Qi, Xiao He, Min Wang, and Xue Zhai. Cross-domain policy adaptation with dynamics alignment. *Neural Networks*, 167:104–117, 2023. 3

Yihong Guo, Yixuan Wang, Yuanyuan Shi, Pan Xu, and Anqi Liu. Off-dynamics reinforcement learning via domain adaptation and reward augmented imitation. *Advances in Neural Information Processing Systems*, 37:136326–136360, 2025. 1, 3

Yihong Guo, Yu Yang, Pan Xu, and Anqi Liu. MOBODY: Model-based off-dynamics offline reinforcement learning. In *The Fourteenth International Conference on Learning Representations*, 2026. URL https://openreview.net/forum?id=7c0YS3cuno. 3

Shengchao Hu, Ziqing Fan, Chaoqin Huang, Li Shen, Ya Zhang, Yanfeng Wang, and Dacheng Tao. Q-value regularized transformer for offline reinforcement learning. *arXiv preprint arXiv:2405.17098*, 2024. 2, 8, 18

Yifeng Jiang, Tingnan Zhang, Daniel Ho, Yunfei Bai, C Karen Liu, Sergey Levine, and Jie Tan. Simgan: Hybrid simulator identification for domain adaptation via adversarial reinforcement learning. In *2021 IEEE International Conference on Robotics and Automation (ICRA)*, pp. 2884–2890. IEEE, 2021. 1

Aviral Kumar, Justin Fu, Matthew Soh, George Tucker, and Sergey Levine. Stabilizing off-policy q-learning via bootstrapping error reduction. *Advances in neural information processing systems*, 32, 2019. 7, 18

Aviral Kumar, Aurick Zhou, George Tucker, and Sergey Levine. Conservative q-learning for offline reinforcement learning. *Advances in Neural Information Processing Systems*, 33:1179–1191, 2020. 7, 18

Eric B Laber, Nick J Meyer, Brian J Reich, Krishna Pacifici, Jaime A Collazo, and John M Drake. Optimal treatment allocations in space and time for on-line control of an emerging infectious disease. *Journal of the Royal Statistical Society Series C: Applied Statistics*, 67(4):743–789, 2018. 1

Sergey Levine. Reinforcement learning and control as probabilistic inference: Tutorial and review. *arXiv preprint arXiv:1805.00909*, 2018. 4

Sergey Levine, Aviral Kumar, George Tucker, and Justin Fu. Offline reinforcement learning: Tutorial, review, and perspectives on open problems. *arXiv preprint arXiv:2005.01643*, 2020. 2

Jinxin Liu, Hongyin Zhang, and Donglin Wang. Dara: Dynamics-aware reward augmentation in offline reinforcement learning. *arXiv preprint arXiv:2203.06662*, 2022. 1, 2, 3, 4, 7, 8, 17, 18

Jinxin Liu, Ziqi Zhang, Zhenyu Wei, Zifeng Zhuang, Yachen Kang, Sibo Gai, and Donglin Wang. Beyond ood state actions: Supported cross-domain offline reinforcement learning. In *Proceedings of the AAAI Conference on Artificial Intelligence*, volume 38, pp. 13945–13953, 2024. 3

Zhishuai Liu and Pan Xu. Distributionally robust off-dynamics reinforcement learning: Provable efficiency with linear function approximation. In *International Conference on Artificial Intelligence and Statistics*, pp. 2719–2727. PMLR, 2024. 1

Zhishuai Liu, Jesse Clifton, Eric B Laber, John Drake, and Ethan X Fang. Deep spatial q-learning for infectious disease control. *Journal of Agricultural, Biological and Environmental Statistics*, 28(4):749–773, 2023. 1

Jiafei Lyu, Chenjia Bai, Jing-Wen Yang, Zongqing Lu, and Xiu Li. Cross-domain policy adaptation by capturing representation mismatch. In *International Conference on Machine Learning*, pp. 33638–33663. PMLR, 2024a. 3

Jiafei Lyu, Kang Xu, Jiacheng Xu, Mengbei Yan, Jingwen Yang, Zongzhang Zhang, Chenjia Bai, Zongqing Lu, and Xiu Li. Odrl: A benchmark for off-dynamics reinforcement learning. *arXiv preprint arXiv:2410.20750*, 2024b. 3

Haoyi Niu, Yiwen Qiu, Ming Li, Guyue Zhou, Jianming Hu, Xianyuan Zhan, et al. When to trust your simulator: Dynamics-aware hybrid offline-and-online reinforcement learning. *Advances in Neural Information Processing Systems*, 35:36599–36612, 2022. 3, 8, 18

Sinno Jialin Pan and Qiang Yang. A survey on transfer learning. *IEEE Transactions on knowledge and data engineering*, 22(10):1345–1359, 2009. 3

Xinlei Pan, Yurong You, Ziyan Wang, and Cewu Lu. Virtual to real reinforcement learning for autonomous driving. *arXiv preprint arXiv:1704.03952*, 2017. 1

Xue Bin Peng, Aviral Kumar, Grace Zhang, and Sergey Levine. Advantage-weighted regression: Simple and scalable off-policy reinforcement learning. *arXiv preprint arXiv:1910.00177*, 2019. 7, 18

Ashish Vaswani, Noam Shazeer, Niki Parmar, Jakob Uszkoreit, Llion Jones, Aidan N Gomez, Łukasz Kaiser, and Illia Polosukhin. Attention is all you need. *Advances in neural information processing systems*, 30, 2017. 4

Guojian Wang, Quinson Hon, Xuyang Chen, and Lin Zhao. Data fusion-enhanced decision transformer for stable cross-domain generalization. *arXiv preprint arXiv:2511.09173*, 2025. 8, 18

Ruhan Wang, Yu Yang, Zhishuai Liu, Dongruo Zhou, and Pan Xu. Return augmented decision transformer for off-dynamics reinforcement learning. *arXiv preprint arXiv:2410.23450*, 2024. 2

Xiaoyu Wen, Chenjia Bai, Kang Xu, Xudong Yu, Yang Zhang, Xuelong Li, and Zhen Wang. Contrastive representation for data filtering in cross-domain offline reinforcement learning. In *Forty-first International Conference on Machine Learning*, 2024. URL https://openreview.net/forum?id=rReWhol66R. 3, 8, 18

Kang Xu, Chenjia Bai, Xiaoteng Ma, Dong Wang, Bin Zhao, Zhen Wang, Xuelong Li, and Wei Li. Cross-domain policy adaptation via value-guided data filtering. *Advances in Neural Information Processing Systems*, 36, 2024. 3

Mengdi Xu, Yikang Shen, Shun Zhang, Yuchen Lu, Ding Zhao, Joshua Tenenbaum, and Chuang Gan. Prompting decision transformer for few-shot policy generalization. In *international conference on machine learning*, pp. 24631–24645. PMLR, 2022. 3

Zhenghai Xue, Qingpeng Cai, Shuchang Liu, Dong Zheng, Peng Jiang, Kun Gai, and Bo An. State regularized policy optimization on data with dynamics shift. *Advances in neural information processing systems*, 36, 2024. 3

Yu Yang and Pan Xu. Pre-trained language models improve the few-shot prompt ability of decision transformer. *Transactions on Machine Learning Research*, 2025. ISSN 2835-8856. URL https://openreview.net/forum?id=k520i3XEMK. 3

Tianhe Yu, Garrett Thomas, Lantao Yu, Stefano Ermon, James Y Zou, Sergey Levine, Chelsea Finn, and Tengyu Ma. Mopo: Model-based offline policy optimization. *Advances in Neural Information Processing Systems*, 33:14129–14142, 2020. 7, 18

Qinqing Zheng, Amy Zhang, and Aditya Grover. Online decision transformer. In *international conference on machine learning*, pp. 27042–27059. PMLR, 2022. 3

Zifeng Zhuang, Dengyun Peng, Ziqi Zhang, Donglin Wang, et al. Reinformer: Max-return sequence modeling for offline rl. *arXiv preprint arXiv:2405.08740*, 2024. 2, 4, 8, 18

A Proof of Theorem 4.5

Lemma A.1 (Corollary 1 of Brandfonbrener et al. (2022))**.** Under the assumptions in Assumption 4.1, there exists a conditioning function such that

$$J^T(\pi^\star) - J^T(\pi_f^{\text{RCSL}}) \leq \epsilon \Big(\frac{1}{\alpha_f} + 3\Big) H^2.$$

Lemma A.2 (Lemma 1 of Brandfonbrener et al. (2022))**.** For any two policies π, π', we have

$$\big\|d_\pi^T - d_{\pi'}^T\big\|_1 \leq 2H \cdot \mathbb{E}_{s \sim d_\pi^T}\big[TV(\pi(\cdot|s)||\hat{\pi}(\cdot|s))\big].$$

We define $d_\beta^{mix} = \frac{N^T}{N^T+N^S}d_\beta^T + \frac{N^S}{N^T+N^S}d_\beta^S$. Define

$$L(\hat{\pi}) = \mathbb{E}_{s \sim d_\beta^{mix}, g \sim P_\beta^T(\cdot|s)}\big[D_{\text{KL}}\big(P_\beta^T(\cdot|s,g)||\hat{\pi}(\cdot|s,g)\big)\big].$$

Theorem A.3. Consider any function $f : \mathcal{S} \to \mathbb{R}$ such that the assumptions in Assumption 4.2 hold. Then for any estimated RCSL policy $\hat{\pi}$ that conditions on f at test time (denoted by $\hat{\pi}_f$), we have

$$J^T(\pi_f^{RCSL}) - J^T(\hat{\pi}_f) \leq \frac{C_f \gamma_f}{\alpha_f} H^2 \sqrt{2L(\hat{\pi})}.$$

Proof. By definition and Lemma A.2, we have

$$J^T(\pi_f) - J^T(\hat{\pi}_f) = H\big(\mathbb{E}_{P_{\pi_f}^T}[r(s,a)] - \mathbb{E}_{P_{\hat{\pi}_f}^T}[r(s,a)]\big)$$

$$\leq H \cdot \|d_{\pi_f} - d_{\hat{\pi}_f}\|_1$$

$$\leq 2 \cdot \mathbb{E}_{s \sim d_{\pi_f}^T}\big[TV(\pi_f(\cdot|s)||\hat{\pi}_f(\cdot|s))\big]H^2.$$

Next, we have

$$2 \cdot \mathbb{E}_{s \sim d_{\pi_f}^T}\big[TV(\pi_f(\cdot|s)||\hat{\pi}_f(\cdot|s))\big]$$

$$= \mathbb{E}_{s \sim d_{\pi_f}^T}\Big[\int_a \big|P_\beta^T(a|s,f(s)) - \hat{\pi}(a|s,f(s))\big|\Big]$$

$$= \mathbb{E}_{s \sim d_{\pi_f}^T}\Big[\frac{P_\beta^T(f(s)|s)}{P_\beta^T(f(s)|s)}\int_a\big|P_\beta^T(a|s,f(s)) - \hat{\pi}(a|s,f(s))\big|\Big]$$

$$\leq 2\frac{C_f}{\alpha_f}\mathbb{E}_{s \sim d_\beta^T, g \sim P_\beta^T(\cdot|s)}\big[TV(P_\beta^T(a|s,f(s))||\hat{\pi}(a|s,f(s)))\big]$$

$$\leq 2\frac{C_f}{\alpha_f}\frac{N^S + N^T}{N^S/\gamma_f + N^T}\cdot\mathbb{E}_{s \sim d_\beta^{mix}, g \sim P_\beta^T(\cdot|s)}\big[TV(P_\beta^T(a|s,f(s))||\hat{\pi}(a|s,f(s)))\big]$$

$$\leq \frac{C_f}{\alpha_f}\frac{N^S + N^T}{N^S/\gamma_f + N^T}\cdot\mathbb{E}_{s \sim d_\beta^{mix}, g \sim P_\beta^T(\cdot|s)}\Big[\sqrt{2KL(P_\beta^T(a|s,f(s))||\hat{\pi}(a|s,f(s)))}\Big]$$

$$\leq \frac{C_f}{\alpha_f}\frac{N^S + N^T}{N^S/\gamma_f + N^T}\sqrt{2L(\hat{\pi})}.$$

$\square$

Proof of Theorem 4.5. Following the same argument in the proof of Corollary 3 in Brandfonbrener et al. (2022), we have

$$J^T(\pi_f^{\text{RCSL}}) - J^T(\hat{\pi}_f) \leq O\Big(2\frac{C_f}{\alpha_f}\frac{N^S + N^T}{N^S/\gamma_f + N^T}H^2\Big(\sqrt{c}\Big(\frac{\log|\Pi|/\delta}{N^S + N^T}\Big)^{1/4} + \sqrt{\epsilon_{\text{approx}}}\Big)\Big).$$

Invoking Lemma A.1, we have

$$J^T(\pi^\star) - J^T(\hat{\pi}_f) \leq O\Big(2\frac{C_f}{\alpha_f}\frac{N^S + N^T}{N^S/\gamma_f + N^T}H^2\Big(\sqrt{c}\Big(\frac{\log|\Pi|/\delta}{N^T + N^S}\Big)^{1/4} + \sqrt{\epsilon_{\text{approx}}}\Big) + \frac{\epsilon}{\alpha_f}H^2\Big).$$

This completes the proof. $\square$

B Detailed Experiment Setting

B.1 Environment and Dataset

In this section, we provide details of the environments and datasets used in our experiments. We evaluate our approaches in the Hopper, Walker2D, and HalfCheetah environments, using the corresponding environments from Gym as our target environments.

B.1.1 Target Environment Dataset Creation

For the target datasets, we construct two distinct datasets: one containing a smaller amount of data (1T) and another with a larger amount (10T). The 10T dataset consists of ten times the number of trajectories as the 1T dataset.

Both Liu et al. (2022) and our work aim to demonstrate the following two key points:

- The 10T dataset represents high-quality data, whereas the 1T dataset represents lower-quality data due to its smaller size.
- Off-dynamics RL algorithms can enhance performance on 1T by effectively leveraging 10S source domain data through appropriate data augmentation.

Liu et al. (2022) creates the 1T dataset by splitting the original target dataset (10T) based on timesteps, selecting the last 1/10 timesteps as 1T. However, this approach introduces unintended bias in the Medium Replay setting, where offline trajectories are collected from a replay buffer in which the behavior policy improves over time. Consequently, the final 1/10 timesteps tend to exhibit a higher average return than the overall 10T dataset, undermining the intended quality distinction between 1T and 10T.

To address this issue and ensure a fair evaluation of off-dynamics RL algorithms, we propose a uniform sampling method across trajectories in the target dataset. This approach ensures that the sampled 1T dataset is a representative subset of the target data, free from biases introduced by timestep-based selection. Notably, our method produces a 1T dataset of lower quality than that of Liu et al. (2022) in medium replay setting. If an off-dynamics RL algorithm can significantly improve performance on our 1T dataset and achieve results comparable to the original 10T dataset, it would serve as a more rigorous evaluation and a stronger indicator of the algorithm's effectiveness.

B.1.2 Source Environment Dataset Creation

We employ BodyMass shift, JointNoise shift to construct the source environments. The following descriptions provide detailed insights into the process of creating these source environments.

- **BodyMass Shift:** The body mass of the agents is modified by adjusting the mass parameters in the Gym environment. Detailed body mass settings are provided in Table 3.
- **JointNoise Shift:** Noise is introduced to the agents' joints by adding perturbations to the actions during source data collection. Specifically, the noise is sampled uniformly from the range $[-0.05, +0.05]$ and applied to the actions when generating the source offline dataset. Detailed joint noise settings are provided in Table 3.

For the source datasets, we utilize the BodyMass Shift and JointNoise Shift datasets from (Liu et al., 2022). Additionally, in our ablation study, we explore variations of BodyMass and JointNoise shifts beyond those specified in Table 3. We also collect medium-level source datasets for the Hopper, Walker2D, and HalfCheetah environments. Behavior policies are generated by training agents with SAC using rlkit (https://github.com/vitchyr/rlkit), with checkpoints used for dataset collection. We construct the Random, Medium, Medium Replay, and Medium Expert datasets, each reflecting different performance levels determined by their corresponding SAC checkpoints. For the JointNoise Shift setting, instead of training a new SAC policy and collecting data through environment interaction, we introduce random noise within a specified range directly to the actions.

Table 3: BodyMass Shift and JointNoise Shift in Hopper, Walker2D and HalfCheetah.

	Hopper		Walker2D		HalfCheetah	
	BodyMass	**JointNoise**	**BodyMass**	**JointNoise**	**BodyMass**	**JointNoise**
Source	mass[-1]=2.5	action[-1]+noise	mass[-1]=1.47	action[-1]+noise	mass[4]=0.5	action[-1]+noise
Target	mass[-1]=5.0	action[-1]+0	mass[-1]=2.94	action[-1]+0	mass[4]=1.0	action[-1]+0

B.2 Baselines

In our experiments, we consider BEAR (Kumar et al., 2019), AWR (Peng et al., 2019), BCQ (Fujimoto et al., 2019), CQL (Kumar et al., 2020), and MOPO (Yu et al., 2020), together with their DARA-augmented variants (Liu et al., 2022), as representative baseline methods. We additionally include recent approaches specifically designed for the off-dynamics setting, including DFDT (Wang et al., 2025), H2O (Niu et al., 2022), and IGDF (Wen et al., 2024). These baselines are compared against DT (Chen et al., 2021), Reinformer (Zhuang et al., 2024), and QT (Hu et al., 2024), as well as our proposed REAG methods.

B.3 Hyperparameters

In this section, we outline the hyperparameters used for our REAG methodologies. The REAG approaches begin with dataset augmentation using either the DARA algorithm ($\text{REAG}^*_{\text{Dara}}$) or the Direct Matching of Return Distributions technique ($\text{REAG}^*_{\text{MV}}$). The augmented dataset is then used to train the DT-type frameworks, which is subsequently evaluated in the target environment. Specifically, for $\text{REAG}^*_{\text{Dara}}$, dataset augmentation follows the DARA algorithm, with its corresponding hyperparameters provided in Table 4. For $\text{REAG}^*_{\text{MV}}$, the augmentation process is described in Section 5.3, where a well-trained Conservative Q-Learning (CQL) model estimates state values, incorporating a clipping mechanism to mitigate extreme values. The hyperparameters for CQL training are provided in Table 5, the clipping ratios are listed in Table 6, and the training parameters for DT, Reinformer, and QT adhere to the settings from their respective original papers.

Table 4: Hyperparameters used in the DARA algorithm.

Hyperparameter	Value
SA Discriminator MLP Layers	4
SAS Discriminator MLP Layers	4
Hidden Dimension	256
Nonlinearity Function	ReLU
Optimizer	RMSprop
Batch Size	256
Learning Rate	3×10^{-4}
Δr Coefficient η	0.1

Table 5: Hyperparameters used in the CQL algorithm.

Hyperparameter	Value
Actor MLP Layers	3
Critic MLP Layers	3
Hidden Dimension	256
Nonlinearity Function	ReLU
Optimizer	Adam
Batch size	256
Discount Factor	0.99
Temperature	1.0
Actor Learning rate	1×10^{-4}
Critic Learning rate	3×10^{-4}

Table 6: Hyperparameters for the Clipping Technique Employed in the $\text{REAG}^*_{\text{MV}}$ Algorithm.

Dataset	Clipping Ratio
Walker2D Random	$0.9 < \theta < 1.25$
Walker2D Medium	$0.9 < \theta < 1.25$
Walker2D Medium Replay	$0.9 < \theta < 1.25$
Walker2D Medium Expert	$0.9 < \theta < 1.25$
Hopper Random	$0.9 < \theta < 1$
Hopper Medium	$0.9 < \theta < 1$
Hopper Medium Replay	$0.9 < \theta < 1$
Hopper Medium Expert	$0.9 < \theta < 1$
HalfCheetah Random	$0.67 < \theta < 1.5$
HalfCheetah Medium	$0.67 < \theta < 1.5$
HalfCheetah Medium Replay	$0.67 < \theta < 1.5$
HalfCheetah Medium Expert	$0.67 < \theta < 1.5$

B.4 Implementation Details and Computational Cost

In all experiments, the uncertainty parameter σ used to determine the clipping bounds is estimated using a fixed budget of 1000 rollouts. This rollout budget is held constant across environments, datasets, and shift settings to ensure consistency.

We also report the wall-clock training cost of CQL to quantify the additional offline computation introduced by our approach. All CQL models are trained under a uniform hardware configuration with an NVIDIA RTX A5000 GPU (24 GB memory) and an AMD Ryzen Threadripper 3960X CPU (24 cores). Training a CQL model on the target dataset requires approximately 2.48 GPU-hours, while training on the source dataset requires approximately 9.39 GPU-hours.

C Experiments

C.1 Additional Experiments Results

This section presents more comprehensive experimental results, including additional variance information.

In Table 2, we provide the performance evaluation of our two return augmentation methods with the standard deviation. In Table 7, we present the experiment results with the 95% confidence interval (CI). The reported CI quantifies the uncertainty of the mean performance and allows assessment of the reliability of the observed improvements. We observe that, in most settings, our proposed methods improve over the corresponding DT-type baselines and the improvement exceeds the CI radius. In some cases, the confidence intervals show limited overlap with those of the baselines, particularly under the Medium-Replay and Medium-Expert settings on Walker2D, Hopper, and HalfCheetah.

In Table 1, we present the partial performance of various algorithms and their DARA variants in the Walker2D medium environment under BodyMass and JointNoise shift settings, considering both limited and sufficient target data scenarios. The complete experimental results are provided in Table 8. Additionally, Table 9 and Table 10 present a comprehensive comparison of different algorithms and their corresponding augmented variants in addressing the off-dynamics problem across various environments and shift settings.

			DT			Reinformer			QT		
			1T10S	$\text{REAG}^{\text{DT}}_{\text{MV}}$	$\text{REAG}^{\text{DT}}_{\text{Dara}}$	1T10S	$\text{REAG}^{\text{Reinf}}_{\text{MV}}$	$\text{REAG}^{\text{Reinf}}_{\text{Dara}}$	1T10S	$\text{REAG}^{\text{QT}}_{\text{MV}}$	$\text{REAG}^{\text{QT}}_{\text{Dara}}$
W2D	M	BM	78.768±1.531	80.857±2.129↑	78.257±3.008↓	80.857±0.632	82.354±1.836↑	80.666±0.627↓	84.325±0.528	84.582±0.629↑	83.068±1.066↓
		JN	71.068±1.269	75.008±2.277↑	71.779±2.118↑	74.748±2.137	75.008±1.224↑	74.268±1.665↓	80.621±1.419	80.904±1.865↑	78.672±2.732↓
	M-R	BM	73.664±2.384	73.708±1.949↑	67.565±0.992↓	67.032±7.160	50.296±17.642↓	66.658±5.342↓	87.292±0.783	87.491±1.522↑	76.169±9.394↓
		JN	58.255±3.949	55.722±3.294↓	62.226±0.475↑	54.801±3.994	47.591±12.718↓	55.438±6.000↑	82.139±1.277	82.363±5.222↑	79.795±5.845↓
	M-E	BM	84.430±1.022	88.235±2.341↑	85.328±1.074↑	83.388±1.001	84.897±1.387↑	83.761±0.912↓	93.082±0.432	92.744±0.619↓	94.578±1.717↑
		JN	115.746±1.385	111.060±2.790↓	111.236±1.135↓	117.360±3.166	118.218±1.813↑	117.765±3.102↑	116.149±2.036	118.564±0.865↑	116.115±2.345↓
Hp	M	BM	34.057±0.220	39.435±1.538↑	37.787±2.376↑	51.357±4.610	59.085±3.465↑	51.771±6.607↑	49.516±12.164	51.796±12.379↑	62.262±6.639↑
		JN	70.685±0.901	70.356±4.540↓	78.325±3.131↑	70.340±5.752	72.346±7.296↑	70.466±4.628↑	68.656±8.788	73.987±10.031↑	68.709±15.096↑
	M-R	BM	64.216±1.867	66.092±0.289↑	60.393±1.348↓	17.534±8.349	20.952±12.159↑	27.238±15.810↑	69.460±17.316	76.287±9.696↑	82.786±14.888↑
		JN	61.870±0.309	77.825±2.034↑	83.525±2.145↑	41.820±19.582	43.985±6.300↑	52.052±12.458↑	93.704±9.384	93.409±5.830↓	51.456±15.106↓
	M-E	BM	33.554±1.050	52.873±0.564↑	33.631±1.993↑	68.973±9.326	64.206±14.988↓	73.363±9.527↑	61.162±4.677	73.952±20.228↑	77.279±23.100↑
		JN	108.254±1.965	109.367±1.346↑	108.261±3.243↑	109.256±0.156	109.472±0.128↑	109.255±0.233↓	109.056±0.266	109.803±0.756↑	109.746±0.957↑
Hc	M	BM	39.954±0.323	40.250±1.131↑	37.599±0.490↓	37.353±0.600	42.451±0.610↑	38.261±1.537↑	44.656±0.798	47.303±0.395↑	46.383±0.444↑
		JN	47.725±0.535	44.149±4.559↓	47.833±0.353↑	48.274±0.237	43.009±0.381↓	48.404±0.209↑	56.213±0.406	52.394±1.754↓	55.026±0.509↓
	M-R	BM	20.966±11.927	27.812±4.042↑	24.059±2.819↑	31.584±1.549	32.114±1.806↑	26.995±5.429↓	41.300±0.977	42.405±0.905↑	41.359±1.223↑
		JN	36.509±5.480	38.417±5.050↑	38.031±4.381↑	40.296±3.618	40.840±3.575↑	38.436±4.192↓	53.763±0.984	53.870±1.218↑	53.257±0.727↓
	M-E	BM	54.981±1.424	56.228±3.637↑	51.357±10.218↓	40.568±1.222	46.048±2.057↑	55.818±2.295↑	71.080±10.927	69.819±6.356↓	76.533±9.959↑
		JN	70.573±10.675	77.762±2.606↑	77.751±3.354↑	76.073±4.814	79.390±0.185↑	78.981±1.487↑	82.961±4.989	83.692±0.868↑	82.148±3.424↓

Table 7: Performance evaluation of two return augmentation methods, $\text{REAG}^{*}_{\text{MV}}$ and $\text{REAG}^{*}_{\text{Dara}}$, integrated with **DT**, **Reinformer**, and **QT** frameworks in off-dynamics scenarios with 95% Confidence Interval (CI). The experiments are conducted in the **Walker2D (W2D)**, **Hopper (Hp)**, and **HalfCheetah (Hc)** environments under the **Medium (M)**, **Medium-Replay (M-R)**, and **Medium-Expert (M-E)** settings. The source environment is modified using two shift conditions: **BodyMass shift (BM)** and **JointNoise shift (JN)**. For reference, the table also includes the performance of the original DT-type methods without augmentation, displayed in **gray** font. Performance changes due to augmentation are indicated with red upward arrows (↑) for improvements and green downward arrows (↓) for degradations compared to the original DT-type methods. All reported values are averaged over five random seeds (0, 1012, 2024, 3036, 4048).

C.2 Ablation Study

C.2.1 Complex Dynamics Shifts

To evaluate the behavior of the proposed method under more complex dynamics shifts, we conduct additional ablation studies on the `HalfCheetah` environment with the following modifications:

- Kinematic Shift. The rotation range of the back thigh joint is modified from the default interval $[-0.52, 1.05]$ to a substantially reduced range $[-0.0052, 0.0105]$. This change constrains the feasible joint motion and alters the transition dynamics by limiting the agent's actuation capability.

		BEAR			AWR			BCQ			CQL		
		M	M-R	M-E	M	M-R	M-E	M	M-R	M-E	M	M-R	M-E
W2D	**1T**	$4.638_{\pm3.882}$	$0.777_{\pm0.105}$	$9.267_{\pm1.692}$	$68.023_{\pm1.687}$	$28.426_{\pm2.974}$	$100.566_{\pm0.513}$	$62.567_{\pm2.459}$	$60.638_{\pm0.683}$	$101.610_{\pm1.309}$	$65.618_{\pm2.818}$	$57.402_{\pm6.161}$	$101.611_{\pm0.143}$
	10T	$13.143_{\pm3.016}$	$5.852_{\pm0.168}$	$21.383_{\pm1.237}$	$78.060_{\pm0.772}$	$58.286_{\pm1.684}$	$109.154_{\pm0.976}$	$74.735_{\pm1.184}$	$64.735_{\pm2.555}$	$101.840_{\pm1.962}$	$78.191_{\pm1.839}$	$80.145_{\pm2.286}$	$101.840_{\pm0.467}$
Hp	**1T**	$8.770_{\pm0.402}$	$5.264_{\pm0.283}$	$31.968_{\pm1.213}$	$55.269_{\pm2.254}$	$54.259_{\pm1.295}$	$54.098_{\pm1.165}$	$63.308_{\pm0.418}$	$68.448_{\pm0.251}$	$62.287_{\pm1.689}$	$74.489_{\pm1.061}$	$71.401_{\pm2.106}$	$82.071_{\pm0.483}$
	10T	$20.398_{\pm2.102}$	$5.554_{\pm0.842}$	$88.236_{\pm2.192}$	$64.494_{\pm2.217}$	$57.548_{\pm1.778}$	$105.361_{\pm1.392}$	$73.462_{\pm2.527}$	$60.385_{\pm0.418}$	$102.775_{\pm1.912}$	$82.945_{\pm0.323}$	$73.168_{\pm2.712}$	$102.071_{\pm1.759}$
Hc	**1T**	$2.659_{\pm0.167}$	$1.602_{\pm0.275}$	$3.089_{\pm0.104}$	$41.672_{\pm0.732}$	$28.023_{\pm4.027}$	$90.168_{\pm1.398}$	$41.051_{\pm2.908}$	$25.828_{\pm6.142}$	$60.173_{\pm4.175}$	$44.393_{\pm0.263}$	$26.955_{\pm1.274}$	$61.621_{\pm13.093}$
	10T	$10.657_{\pm0.271}$	$19.588_{\pm0.453}$	$16.160_{\pm0.208}$	$42.209_{\pm0.611}$	$41.041_{\pm0.729}$	$90.212_{\pm2.259}$	$46.188_{\pm0.423}$	$38.575_{\pm2.060}$	$95.535_{\pm4.042}$	$49.382_{\pm0.338}$	$46.966_{\pm0.372}$	$87.683_{\pm7.753}$
		MOPO			**DT**			**Reinformer**			**QT**		
		M	M-R	M-E	M	M-R	M-E	M	M-R	M-E	M	M-R	M-E
W2D	**1T**	$20.953_{\pm2.715}$	$20.313_{\pm3.488}$	$20.569_{\pm0.983}$	$67.261_{\pm2.316}$	$34.482_{\pm5.890}$	$107.171_{\pm1.611}$	$79.034_{\pm1.506}$	$38.072_{\pm9.174}$	$103.284_{\pm5.437}$	$81.756_{\pm1.671}$	$67.546_{\pm9.505}$	$111.722_{\pm1.398}$
	10T	$22.261_{\pm2.811}$	$18.529_{\pm1.760}$	$21.196_{\pm3.103}$	$79.697_{\pm3.348}$	$68.528_{\pm1.924}$	$108.622_{\pm1.815}$	$81.377_{\pm1.903}$	$68.168_{\pm2.661}$	$109.845_{\pm0.726}$	$88.262_{\pm12.886}$	$85.092_{\pm8.727}$	$111.394_{\pm0.469}$
Hp	**1T**	$31.038_{\pm2.868}$	$5.849_{\pm0.146}$	$35.099_{\pm1.212}$	$66.073_{\pm1.745}$	$61.686_{\pm2.592}$	$100.719_{\pm1.679}$	$74.737_{\pm4.807}$	$36.008_{\pm6.575}$	$60.753_{\pm14.433}$	$70.927_{\pm6.482}$	$83.406_{\pm4.734}$	$108.225_{\pm5.596}$
	10T	$32.769_{\pm1.788}$	$8.638_{\pm1.395}$	$36.161_{\pm2.204}$	$85.589_{\pm5.311}$	$69.701_{\pm5.317}$	$108.087_{\pm1.049}$	$77.792_{\pm4.652}$	$39.856_{\pm12.334}$	$79.389_{\pm28.054}$	$90.176_{\pm0.186}$	$100.321_{\pm1.121}$	$112.908_{\pm3.154}$
Hc	**1T**	$64.329_{\pm2.096}$	$12.277_{\pm1.953}$	$25.055_{\pm7.834}$	$41.204_{\pm0.430}$	$15.164_{\pm4.847}$	$77.500_{\pm3.323}$	$42.958_{\pm0.065}$	$18.493_{\pm1.584}$	$72.085_{\pm3.491}$	$50.464_{\pm0.127}$	$32.318_{\pm2.435}$	$87.854_{\pm6.657}$
	10T	$65.863_{\pm1.289}$	$59.724_{\pm1.056}$	$28.221_{\pm6.078}$	$42.273_{\pm0.379}$	$34.508_{\pm1.482}$	$82.844_{\pm7.635}$	$43.243_{\pm0.262}$	$39.434_{\pm0.362}$	$87.378_{\pm3.340}$	$51.284_{\pm0.605}$	$49.587_{\pm0.334}$	$94.116_{\pm0.321}$

Table 8: Performance comparison of algorithms on the **1T**, **10T**, and **1T10S** datasets. In this study, **1T10S(B)** refers to the source dataset under the **BodyMass shift** setting, while **1T10S(J)** corresponds to the source dataset under the **JointNoise shift** setting. The experiments are conducted in the **Walker2D (W2D)**, **Hopper (Hp)**, and **HalfCheetah (Hc)** using the **Medium (M)**, **Medium Replay (M-R)**, and **Medium Expert (M-E)** datasets. All reported values are averaged over five seeds (0, 1012, 2024, 3036, 4048).

		BEAR	AWR	BCQ	CQL	MOPO	D-BEAR	D-AWR	D-BCQ	D-CQL	D-MOPO	DFDT	H2O	IGDF
Walker2D M	**BM**	5.776 ± 1.653	77.442 ± 0.340	70.681 ± 0.539	73.317 ± 1.368	21.617 ± 1.277	6.516 ± 3.220	78.004 ± 0.911	72.023 ± 0.695	74.276 ± 2.582	21.621 ± 1.063	80.693 ± 0.401	63.031 ± 8.582	78.271 ± 2.091
	JN	4.926 ± 1.418	67.636 ± 1.468	62.696 ± 1.037	68.962 ± 0.865	23.552 ± 1.063	6.933 ± 1.884	64.303 ± 0.513	60.681 ± 1.118	69.141 ± 0.944	23.570 ± 0.665	76.373 ± 5.636	72.849 ± 13.762	80.549 ± 2.811
Walker2D M-R	**BM**	0.067 ± 4.951	47.033 ± 2.278	50.714 ± 1.918	54.753 ± 0.335	11.563 ± 2.751	1.078 ± 2.083	32.008 ± 1.286	51.447 ± 3.108	57.432 ± 0.764	12.129 ± 2.755	71.670 ± 10.678	56.110 ± 9.162	62.494 ± 4.081
	JN	0.474 ± 0.719	31.623 ± 2.551	50.601 ± 1.611	50.600 ± 1.589	11.379 ± 0.596	0.384 ± 3.823	36.807 ± 2.442	50.714 ± 0.876	51.742 ± 1.061	15.389 ± 0.559	71.236 ± 4.658	55.228 ± 6.383	66.834 ± 7.751
Walker2D M-E	**BM**	19.799 ± 3.116	110.324 ± 1.053	112.343 ± 1.488	107.187 ± 3.209	18.324 ± 0.708	17.491 ± 2.844	109.743 ± 2.632	113.069 ± 1.602	105.401 ± 2.186	20.741 ± 0.399	108.086 ± 0.270	83.768 ± 14.152	111.936 ± 0.612
	JN	14.225 ± 1.338	104.662 ± 2.370	112.926 ± 1.491	104.019 ± 0.294	17.429 ± 0.639	14.203 ± 1.602	108.915 ± 1.915	111.249 ± 1.092	108.236 ± 1.206	19.325 ± 3.119	108.390 ± 0.707	95.862 ± 6.778	111.226 ± 1.229
Hopper M	**BM**	22.436 ± 0.103	25.843 ± 0.325	24.853 ± 1.615	49.094 ± 2.207	20.765 ± 3.350	25.608 ± 1.063	26.594 ± 1.267	26.487 ± 1.366	45.101 ± 0.342	21.495 ± 0.848	66.133 ± 3.840	100.754 ± 2.287	75.326 ± 8.112
	JN	8.536 ± 1.965	57.021 ± 0.938	74.559 ± 0.605	71.495 ± 0.126	23.556 ± 1.327	10.576 ± 2.052	61.463 ± 0.702	74.853 ± 0.626	63.611 ± 1.136	24.992 ± 0.944	59.760 ± 2.184	101.244 ± 0.452	78.467 ± 2.849
Hopper M-R	**BM**	6.282 ± 0.132	55.607 ± 2.310	64.519 ± 0.813	66.455 ± 0.636	5.504 ± 1.701	2.619 ± 0.128	44.883 ± 1.595	64.168 ± 0.291	68.163 ± 0.559	5.482 ± 1.061	74.720 ± 11.472	97.538 ± 3.471	95.655 ± 2.795
	JN	1.841 ± 3.814	37.821 ± 1.205	65.103 ± 0.703	61.302 ± 1.207	5.498 ± 0.568	5.637 ± 0.291	63.937 ± 3.879	64.519 ± 1.102	63.178 ± 1.218	6.147 ± 0.157	74.720 ± 11.472	98.988 ± 1.445	95.230 ± 3.558
Hopper M-E	**BM**	22.934 ± 3.022	57.595 ± 0.612	109.367 ± 0.834	70.467 ± 2.712	30.541 ± 3.616	31.090 ± 0.463	78.262 ± 0.239	110.014 ± 2.153	72.149 ± 1.934	30.540 ± 0.842	70.703 ± 10.556	108.872 ± 2.802	105.465 ± 8.805
	JN	39.031 ± 1.079	74.708 ± 1.889	108.639 ± 2.028	72.512 ± 0.781	30.537 ± 0.842	33.052 ± 0.385	60.952 ± 0.879	111.587 ± 1.602	94.128 ± 1.213	32.589 ± 1.985	74.306 ± 18.284	109.457 ± 2.819	99.057 ± 23.594
HalfCheetah M	**BM**	5.431 ± 1.518	42.293 ± 0.862	39.835 ± 0.427	37.081 ± 0.358	58.457 ± 1.449	6.009 ± 1.705	41.800 ± 0.830	39.333 ± 0.506	37.189 ± 0.218	59.311 ± 0.949	43.580 ± 0.157	55.566 ± 1.803	47.239 ± 0.131
	JN	1.948 ± 1.058	41.992 ± 0.762	50.511 ± 0.371	49.046 ± 0.420	61.073 ± 0.315	2.901 ± 0.402	42.545 ± 0.731	52.149 ± 0.457	49.284 ± 0.570	61.447 ± 0.734	43.760 ± 0.245	57.924 ± 1.489	46.647 ± 0.289
HalfCheetah M-R	**BM**	7.425 ± 1.307	15.988 ± 5.339	32.553 ± 1.258	37.508 ± 0.520	50.429 ± 1.306	4.909 ± 0.562	17.918 ± 3.701	32.095 ± 1.258	37.721 ± 0.440	52.609 ± 0.621	36.626 ± 1.047	57.835 ± 1.805	46.365 ± 0.239
	JN	18.337 ± 0.498	31.742 ± 4.199	46.567 ± 2.563	51.566 ± 0.246	51.918 ± 1.584	17.929 ± 0.479	38.125 ± 1.775	49.066 ± 0.645	52.991 ± 0.438	51.258 ± 1.709	31.193 ± 2.018	57.734 ± 1.061	46.611 ± 0.157
HalfCheetah M-E	**BM**	4.356 ± 0.431	88.155 ± 1.836	61.771 ± 4.610	61.104 ± 4.131	51.040 ± 4.461	2.948 ± 0.691	89.201 ± 2.419	63.465 ± 3.303	62.665 ± 5.326	56.616 ± 2.609	78.093 ± 15.794	58.192 ± 2.092	48.112 ± 0.230
	JN	3.195 ± 0.391	88.647 ± 2.669	62.486 ± 10.025	84.090 ± 1.109	54.630 ± 10.104	8.789 ± 0.271	89.220 ± 1.800	71.007 ± 4.201	84.210 ± 0.506	60.014 ± 7.011	82.476 ± 2.441	60.230 ± 1.072	48.192 ± 0.255

Table 9: Performance comparison of conventional offline reinforcement learning methods—BEAR, AWR, BCQ, CQL, and MOPO—and their DARA-augmented variants, together with recent dynamics-aware baselines (DFDT, H2O, and IGDF), under **BodyMass** and **JointNoise** distribution shifts on the **Walker2D**, **Hopper**, and **HalfCheetah** environments. All methods are evaluated on the **Medium (M)**, **Medium-Replay (M-R)**, and **Medium-Expert (M-E)** splits of the **1T10S** dataset, which consists of one target dataset (**1T**) and ten source datasets (**10S**). **D-XX** denotes the DARA-augmented variant of algorithm **XX**. DFDT, H2O, and IGDF are included as representative off-dynamics baselines and are evaluated under identical experimental settings.

These settings introduce structured changes to the underlying system dynamics beyond those considered in the main experiments. The corresponding results are reported in Table 11. Under the kinematic shift, all methods achieve comparable performance across DT, Reinformer, and QT, indicating that restricting joint motion primarily limits action expressiveness without fundamentally destabilizing the learned policies. In this setting, the proposed methods consistently match or improve upon their corresponding baselines, with $\text{REAG}^{\text{QT}}_{\text{MV}}$ yielding the strongest performance.

		DT	Reinformer	QT	$\text{REAG}_{\text{MV}}^{\text{DT}}$	$\text{REAG}_{\text{MV}}^{\text{Reinf}}$	$\text{REAG}_{\text{MV}}^{\text{QT}}$	$\text{REAG}_{\text{Dara}}^{\text{DT}}$	$\text{REAG}_{\text{Dara}}^{\text{Reinf}}$	$\text{REAG}_{\text{Dara}}^{\text{QT}}$
Walker2D M	BM	78.768 ± 1.233	80.857 ± 0.509	84.325 ± 0.425	80.857 ± 1.715	82.354 ± 1.479	84.582 ± 0.507	78.257 ± 2.423	80.666 ± 0.505	83.068 ± 0.859
	JN	71.068 ± 1.022	74.748 ± 1.721	80.621 ± 1.143	75.008 ± 1.834	75.008 ± 0.986	80.904 ± 1.502	71.779 ± 1.706	74.268 ± 1.341	78.672 ± 2.201
Walker2D M-R	BM	73.664 ± 1.920	67.032 ± 5.767	87.292 ± 0.631	73.708 ± 1.570	50.296 ± 14.211	87.491 ± 1.226	67.565 ± 0.799	66.658 ± 4.303	76.169 ± 7.567
	JN	58.255 ± 3.181	54.801 ± 3.217	82.139 ± 1.029	55.722 ± 2.653	47.591 ± 10.244	82.363 ± 4.206	62.226 ± 0.383	55.438 ± 4.833	79.795 ± 4.708
Walker2D M-E	BM	84.430 ± 0.823	83.388 ± 0.806	93.082 ± 0.348	88.235 ± 1.886	84.897 ± 1.117	92.744 ± 0.499	85.328 ± 0.865	83.761 ± 0.735	94.578 ± 1.383
	JN	115.746 ± 1.116	117.360 ± 2.550	116.149 ± 1.640	111.060 ± 2.247	118.218 ± 1.460	118.564 ± 0.697	111.236 ± 0.914	117.765 ± 2.499	116.115 ± 1.889
Hopper M	BM	34.057 ± 0.177	51.357 ± 3.713	49.516 ± 9.798	39.435 ± 1.239	59.085 ± 2.791	51.796 ± 9.971	37.787 ± 1.914	51.771 ± 5.322	62.262 ± 5.348
	JN	70.685 ± 0.726	70.340 ± 4.633	68.656 ± 7.079	70.356 ± 3.657	72.346 ± 5.877	73.987 ± 8.080	78.325 ± 2.522	70.466 ± 3.728	68.709 ± 12.160
Hopper M-R	BM	64.216 ± 1.504	17.534 ± 6.725	69.460 ± 13.948	66.092 ± 0.233	20.952 ± 9.794	76.287 ± 7.810	60.393 ± 1.086	27.238 ± 12.735	82.786 ± 11.992
	JN	61.870 ± 0.249	41.820 ± 15.773	93.704 ± 7.559	77.825 ± 1.638	43.985 ± 5.075	93.409 ± 4.696	83.525 ± 1.728	52.052 ± 10.035	51.456 ± 12.168
Hopper M-E	BM	33.554 ± 0.846	68.973 ± 7.512	61.162 ± 3.767	52.873 ± 0.454	64.206 ± 12.073	73.952 ± 16.294	33.631 ± 1.605	73.363 ± 7.674	77.279 ± 18.607
	JN	108.254 ± 1.583	109.256 ± 0.126	109.056 ± 0.214	109.367 ± 1.084	109.472 ± 0.103	109.803 ± 0.609	108.261 ± 2.612	109.255 ± 0.188	109.746 ± 0.771
HalfCheetah M	BM	39.954 ± 0.260	37.353 ± 0.483	44.656 ± 0.643	40.250 ± 0.911	42.451 ± 0.491	47.303 ± 0.318	37.599 ± 0.395	38.261 ± 1.238	46.383 ± 0.358
	JN	47.725 ± 0.431	48.274 ± 0.191	56.213 ± 0.327	44.149 ± 3.672	43.009 ± 0.307	52.394 ± 1.413	47.833 ± 0.284	48.404 ± 0.168	55.026 ± 0.410
HalfCheetah M-R	BM	20.966 ± 9.607	31.584 ± 1.248	41.300 ± 0.787	27.812 ± 3.256	32.114 ± 1.455	42.405 ± 0.729	24.059 ± 2.271	26.995 ± 4.373	41.359 ± 0.985
	JN	36.509 ± 4.414	40.296 ± 2.914	53.763 ± 0.793	38.417 ± 4.068	40.840 ± 2.880	53.870 ± 0.981	38.031 ± 3.529	38.436 ± 3.377	53.257 ± 0.586
HalfCheetah M-E	BM	54.981 ± 1.147	40.568 ± 0.984	71.008 ± 8.802	56.228 ± 2.930	46.048 ± 1.657	69.819 ± 5.120	51.357 ± 8.231	55.818 ± 1.849	76.533 ± 8.022
	JN	70.573 ± 8.599	76.073 ± 3.878	82.961 ± 4.019	77.762 ± 2.099	79.390 ± 0.149	83.692 ± 0.699	77.751 ± 2.702	78.981 ± 1.198	82.148 ± 2.758

Table 10: Performance comparison of traditional offline reinforcement learning algorithms, including DT, Reinformer and QT, along with our proposed methods $\text{REAG}_{\text{MV}}^{\text{DT}}$, $\text{REAG}_{\text{Dara}}^{\text{DT}}$, $\text{REAG}_{\text{MV}}^{\text{Reinf}}$, $\text{REAG}_{\text{Dara}}^{\text{Reinf}}$, $\text{REAG}_{\text{MV}}^{\text{QT}}$ and $\text{REAG}_{\text{Dara}}^{\text{QT}}$ under BodyMass and JointNoise distribution shifts in the **Walker2D**, **Hopper**, and **HalfCheetah** environments. Evaluations are conducted using the **Medium (M)**, **Medium Replay (M-R)**, and **Medium Expert (M-E)** settings of the **1T10S** dataset. The **1T10S** dataset comprises a **1T** (target) dataset and a **10S** (source) dataset.

Method	Baseline	$\text{REAG}_{\text{MV}}^{*}$	$\text{REAG}_{\text{Dara}}^{*}$
DT	42.277 ± 1.062	42.752 ± 2.387	41.257 ± 4.437
Reinformer	42.929 ± 0.539	42.826 ± 0.558	43.092 ± 0.442
QT	43.968 ± 2.037	47.698 ± 0.211	43.896 ± 3.677

Table 11: Performance comparison of traditional offline reinforcement learning algorithms, including DT, Reinformer and QT, along with our proposed methods $\text{REAG}_{\text{MV}}^{\text{DT}}$, $\text{REAG}_{\text{Dara}}^{\text{DT}}$, $\text{REAG}_{\text{MV}}^{\text{Reinf}}$, $\text{REAG}_{\text{Dara}}^{\text{Reinf}}$, $\text{REAG}_{\text{MV}}^{\text{QT}}$ and $\text{REAG}_{\text{Dara}}^{\text{QT}}$ under Kinematic shifts in **HalfCheetah** environment. Evaluations are conducted using the **Medium (M)** setting of the **1T10S** dataset. The **1T10S** dataset comprises a **1T** (target) dataset and a **10S** (source) dataset.

C.2.2 Sensitivity to Q-Function Quality

$\text{REAG}_{\text{MV}}^{*}$ uses learned Q-functions for return relabeling. To evaluate its sensitivity to Q-function quality, we vary two factors in CQL training: (i) the conservative regularization coefficient α and (ii) the number of target samples used to train the critic.

All experiments are conducted on Walker2D-Medium with BodyMass dynamics shift. For each setting, CQL critics trained under different α values and dataset sizes are used for return relabeling in $\text{REAG}_{\text{MV}}^{*}$, while all other components are kept fixed.

As shown in Figure 7, $\text{REAG}_{\text{MV}}^{*}$ achieves similar performance across a broad range of α values and training sample sizes. Although CQL training becomes less stable under strong regularization or limited data, the final policy performance varies only marginally. This suggests that $\text{REAG}_{\text{MV}}^{*}$ is not highly sensitive to the quality of the learned Q-functions.

C.3 Gaussian Approximation of Return Distributions

Our approach models trajectory-level returns using a Gaussian distribution. This assumption is supported by empirical analysis on standard offline RL benchmarks.
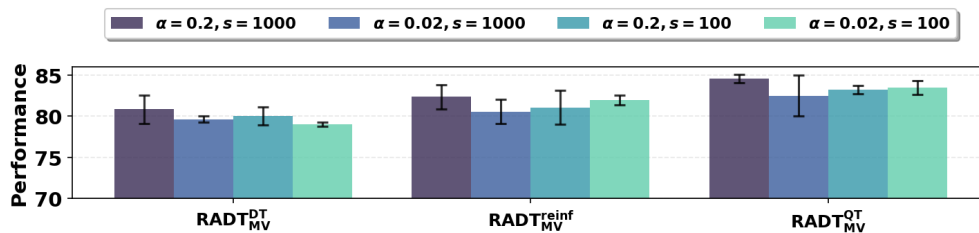
Figure 7: Performance of $\mathbf{REAG}^*_{\mathrm{MV}}$ under different CQL training settings on the **Walker2D-Medium** environment with **BodyMass** dynamics shift.
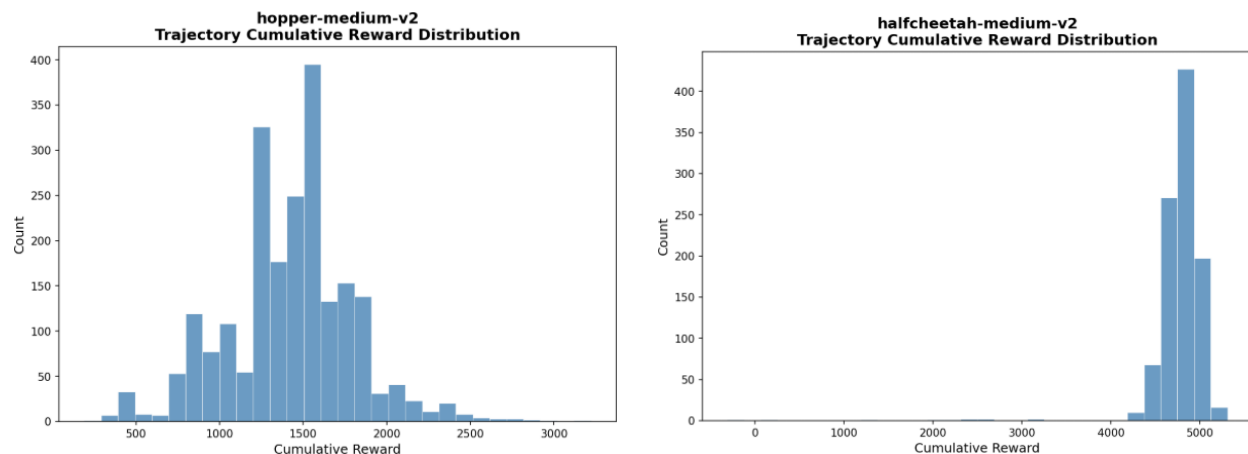

Figure 8: Empirical return distributions of trajectory-level cumulative rewards in the D4RL medium datasets for Hopper and HalfCheetah.

We examine the D4RL medium datasets, which are collected using medium-performance SAC policies. For the Hopper and HalfCheetah environments, we compute the cumulative reward of each trajectory and analyze the empirical return distributions. As shown in Figure 8, the resulting histograms are unimodal and approximately symmetric, without pronounced skewness or heavy tails.

These characteristics indicate that a Gaussian distribution provides a reasonable approximation of the observed return distributions in these datasets. While this assumption is not expected to hold in all settings, it is appropriate for the benchmarks considered in this work.

D   Analysis of Failure Cases

REAG improves target-domain policy learning by augmenting training with relabeled source trajectories. Its effectiveness depends on the degree of alignment between the source and target domains, particularly with respect to state–action occupancy. This dependency is formalized in our theoretical analysis through the domain occupancy overlap coefficient (Assumption 4.2 and Remark 4.6), which characterizes the conditions under which source data can provide reliable information for the target task.

When the source–target occupancy overlap is limited, return relabeling may introduce bias. In this regime, relabeled source trajectories can distort the estimation of return statistics and value functions, resulting in degraded downstream performance. This behavior is observed for Reinformer on the Walker2D Medium-Replay dataset under both BodyMass and JointNoise dynamics shifts, where REAG shows limited effectiveness and may negatively affect performance.

A contributing factor is the structure of Medium-Replay datasets, which are generated from mixtures of behavior policies and exhibit substantial heterogeneity and multi-modality in both state visitation and

return distributions. In such settings, the target subset (1T) is often insufficient to reliably characterize the target return distribution, which can deviate from a Gaussian form in parts of the data. Consequently, the return statistics and Q-function estimates used for relabeling become noisy, reducing the reliability of return augmentation.

Based on these observations, REAG is best suited for settings with sufficient source–target occupancy overlap and relatively stable return distributions, such as Medium and Medium-Expert datasets. For highly heterogeneous replay datasets, aggregation-based variants such as $\text{REAG}^*_{\text{Dara}}$ or disabling return relabeling may be more appropriate.

E Additional Theoretical Results

Recall that in Section 4.3, we assume a single behavior policy to collect offline dataset under both source and target environments. This simple setting is studied to provide principled motivation and conceptual guidance for the proposed method. While in practical implementations, we use different policies to collect the source and target datasets, leading to a gap between our theoretical analysis and practical implementation. In this section, we generalize our theoretical analysis and results to the case where the source dataset and target dataset are collected by different behavior policies, thus aligning with our empirical implementation.

We generate the source dataset D^S by β_S and target dataset D^T by β_T, and denote their sample sizes as N^S and N^T. Denote the occupancy measure over state induced by β_S under P^S as $d^S_{\beta_S}$ and by β_T under P^T as $d^T_{\beta_T}$. Define the mixture occupancy measure as $d^{mix} := \frac{N^T}{N^S+N^T}d^T_{\beta_T} + \frac{N^S}{N^S+N^T}d^S_{\beta_S}$, and the mixture policy as $\beta := \frac{N^T}{N^S+N^T}\beta_T + \frac{N^S}{N^S+N^T}\beta_S$. For simplicity, we denote $c := \frac{N^S}{N^S+N^T}\beta_S$ and thus $\beta = c\beta_S + (1-c)\beta_T$. Recall the definition $P^T_{\beta_T}(g|s,a)$ is the distribution over return induced by β_T under P^T. We define the goal policy of interest as

$$\pi_f(a|s) = \frac{\beta(a|s)P^T_{\beta_T}(g=f(s)|s,a)}{\sum_{a'\in\mathcal{A}}P^T_{\beta_T}(g=f(s)|s,a')\beta(a'|s)}.$$

We define $P^T_{\beta,\beta_T}(\cdot|s) = \sum_{a'\in\mathcal{A}}P^T_{\beta_T}(g=f(s)|s,a')\beta(a'|s)$.

We make the following assumptions, which corresponding to Assumption 4.1, Assumption 4.2 and Assumption 4.3 in the main text.

Assumption E.1. (1) (Near determinism) $P^T(r \neq r(s,a)$ or $s' \neq \xi(s,a)|s,a) \leq \epsilon$ at all s,a for some functions ξ and r. (2) (Consistency of f) $f(s) = f(s') + r$ for all s.

Assumption E.2. For all s we assume (1) (Bounded occupancy mismatch) $P^T_{\pi_f}(s) \leq C_f P^T_{\beta_T}(s)$; (2) (Return coverage) (Return coverage) $\int_a \beta_S(a|s)P^T_{\beta_T}(\cdot|s,a)da \geq \alpha_f$ and $\int_a \beta_T(a|s)P^T_{\beta_T}(\cdot|s,a)da \geq \alpha_f$; and (3) (Domain occupancy overlap) $d^T_{\beta_T}(s) \leq \gamma_f d^S_{\beta_S}(s)$.

Assumption E.3. (1) The policy class Π is finite. (2)$|\log\pi(a|s,g) - \log\pi(a'|s',g')| \leq c$ for any (a,s,g,a',s',g') and all $\pi \in \Pi$. (3) The approximation error is bounded by ϵ_{approx}, i.e., $\min_{\pi\in\Pi}L(\pi) \leq \epsilon_{\text{approx}}$.

π_f is the policy we want to learn. In the following theorem, we show that this policy is near optimal under the target environment.

Theorem E.4. Under the assumptions in Assumption 4.1, there exists a conditioning function such that

$$J^T(\pi^\star) - J^T(\pi_f) \leq \epsilon\Big(\frac{1}{\alpha_f} + 3\Big)H^2.$$

Proof. The general proof idea follows the proof of Corollary 1 of Brandfonbrener et al. (2022). But since our policy π_f is not a classical RCSL policy, we need careful analysis on the derivation.

Let $g(s_1, a_{1:H})$ be the value of return by rolling out the open loop sequence of actions $a_{1:H}$ under the deterministic dynamics induced by P^T and r. Then we have

$$
\begin{aligned}
\mathbb{E}_{s_1}[f(s_1)] - J(\pi_f) &= \mathbb{E}_{s_1}[\mathbb{E}_{\pi_f | s_1}[f(s_1) - g_1]] \\
&= \mathbb{E}_{s_1}[\mathbb{E}_{a_{1:H} \sim \pi_f | s_1}[f(s_1) - g(s_1, a_{1:H})]] + \mathbb{E}_{s_1}[\mathbb{E}_{a_{1:H} \sim \pi_f | s_1}[g(s_1, a_{1:H}) - g_1]] \\
&\leq \mathbb{E}_{s_1}[\mathbb{E}_{a_{1:H} \sim \pi_f | s_1}[f(s_1) - g(s_1, a_{1:H})]] + \epsilon H^2
\end{aligned}
\tag{E.1}
$$

where the last step follows by bounding the magnitude of the difference between g_1 and $g(s_1, a_{1:H})$ by H and applying a union bound over the H steps in the trajectory. Now we consider the first term. Again bounding the magnitude of the difference by H we get that

$$
\mathbb{E}_{s_1}[\mathbb{E}_{a_{1:H} \sim \pi_f | s_1}[f(s_1) - g(s_1, a_{1:H})]] \leq \mathbb{E}_{s_1} \int_{a_{1:H}} P_{\pi_f}^T(a_{1:H}|s_1) \mathbb{1}\{g(s_1, a_{1:H}) \neq f(s_1)\} H.
\tag{E.2}
$$

To bound this term, we will more carefully consider what happens under the distribution $P_{\pi_f}^T$. To simplify notion, let $\bar{s}_t = P^T(s_1, a_{1:t-1})$ be the result of following the deterministic dynamics defined by ξ up until step t. Expanding it out, applying the near determinism, the consistency of f, the coverage assumption, we have

$$
\begin{aligned}
P_{\pi_f}^T(a_{1:H}|s_1) &= \pi_f(a_1|s_1) \int_{s_2} P^T(s_2|s_1, a_1) P_{\pi_f}^T(a_{2:H}|s_1, s_2) \\
&\leq \pi_f(a_1|s_1) P_{\pi_f}(a_{2:H}|s_1, \bar{s}_2) + \epsilon \\
&= \beta(a_1|s_1) \frac{P_{\beta_T}^T(g_1 = f(s_1)|s_1, a_1)}{\sum_{a' \in \mathcal{A}} P_{\beta_T}^T(g_1 = f(s_1)|s_1, a_1) \beta(a'|s)} P_{\pi_f}(a_{2:H}|s_1, \bar{s}_2) + \epsilon \\
&= \beta(a_1|s_1) \frac{\epsilon + P_{\beta_T}^T(g_1 - r(s_1, a_1) = f(s_1) - r(s_1, a_1)|s_1, a_1, \bar{s}_2)}{\sum_{a' \in \mathcal{A}} P_{\beta_T}^T(g_1 = f(s_1)|s_1, a_1) \beta(a'|s)} P_{\pi_f}(a_{2:H}|s_1, \bar{s}_2) + \epsilon \\
&= \beta(a_1|s_1) \frac{\epsilon + P_{\beta_T}^T(g_2 = f(\bar{s}_2)|\bar{s}_2)}{P_{\beta, \beta_T}^T(g_1 = f(s_1)|s_1)} P_{\pi_f}(a_{2:H}|s_1, \bar{s}_2) + \epsilon \\
&\leq \beta(a_1|s_1) \frac{P_{\beta_T}^T(g_2 = f(\bar{s}_2)|\bar{s}_2)}{P_{\beta, \beta_T}^T(g_1 = f(s_1)|s_1)} P_{\pi_f}(a_{2:H}|s_1, \bar{s}_2) + \epsilon(1/\alpha_f + 1) \\
&\leq \beta(a_1|s_1) \beta(a_2|\bar{s}_2) \frac{P_{\beta_T}^T(g_2 = f(\bar{s}_2)|\bar{s}_2)}{P_{\beta, \beta_T}^T(g_1 = f(s_1)|s_1)} \frac{P_{\beta_T}^T(g_3 = f(\bar{s}_3)|\bar{s}_3)}{P_{\beta, \beta_T}^T(g_2 = f(\bar{s}_2)|\bar{s}_2)} P_{\pi_f}(a_{3:H}|s_1, \bar{s}_3) + 2\epsilon(1/\alpha_f + 1) \\
&\leq \beta(a_1|s_1) \beta(a_2|\bar{s}_2) \cdots \beta(a_H|\bar{s}_H) \frac{P_{\beta_T}^T(g_2 = f(\bar{s}_2)|\bar{s}_2)}{P_{\beta, \beta_T}^T(g_1 = f(s_1)|s_1)} \\
&\quad \cdot \frac{P_{\beta_T}^T(g_3 = f(\bar{s}_3)|\bar{s}_3)}{P_{\beta, \beta_T}^T(g_2 = f(\bar{s}_2)|\bar{s}_2)} \cdots \frac{P_{\beta_T}^T(g_H = f(\bar{s}_H)|\bar{s}_H)}{P_{\beta, \beta_T}^T(g_{H-1} = f(\bar{s}_{H-1})|\bar{s}_{H-1})} + H\epsilon(1/\alpha_f + 1).
\end{aligned}
$$

By the fact that

$$
\begin{aligned}
P_{\beta, \beta_T}^T(g_h = f(\bar{s}_h)|\bar{s}_h) &= \sum_{a' \in \mathcal{A}} P_{\beta_T}^T(g_h = f(\bar{s}_h)|\bar{s}_h, a') \cdot \beta(a'|\bar{s}_h) \\
&= \sum_{a' \in \mathcal{A}} P_{\beta_T}^T(g_h = f(\bar{s}_h)|\bar{s}_h, a') \cdot (c \cdot \beta_S(a'|\bar{s}_h) + (1-c) \cdot \beta_T(a'|\bar{s}_h)) \\
&\geq \sum_{a' \in \mathcal{A}} P_{\beta_T}^T(g_h = f(\bar{s}_h)|\bar{s}_h, a') \cdot (1-c) \cdot \beta_T(a'|\bar{s}_h) \\
&= (1-c) P_{\beta_T}^T(g_h = f(\bar{s}_h)|\bar{s}_h),
\end{aligned}
$$

we have

$$P^T_{\pi_f}(a_{1:H}|s_1) \leq \prod_{t=1}^{H} \beta(a_t|\bar{s}_t) \frac{P^T_{\beta_T}(g_H = f(\bar{s}_H)|\bar{s}_H)}{P^T_{\beta,\beta_T}(g_1 = f(s_1)|s_1)} \frac{1}{(1-c)^H} + H\epsilon(1/\alpha_f + 1)$$

$$= \prod_{t=1}^{H} \beta(a_t|\bar{s}_t) \frac{\mathbb{1}\{g(s_1, a_{1:H}) = f(s_1)\}}{P^T_{\beta,\beta_T}(g_1 = f(s_1)|s_1)} \frac{1}{(1-c)^H} + H\epsilon(1/\alpha_f + 1),$$

where the last step follows from the determinism of the trajectory that determines $\bar{s}_H$ and the consistency of f. Plugging this back into (E.2) and noticing that the two indicator can never both be 1, we have

$$\mathbb{E}_{s_1}[\mathbb{E}_{a_{1:H} \sim \pi_f|s_1}[f(s_1) - g(s_1, a_{1:H})]] \leq H^2\epsilon(1/\alpha_f + 1).$$

Plugging this back into (E.1) finishes the proof. $\square$

Now we are ready to state and prove our main theorem.

Theorem E.5. There exists a conditioning function f such that Assumptions E.1 and E.2 hold. Further assume Assumption E.3 holds. Then for some $\delta \in (0, 1)$, with probability at least $1 - \delta$, we have

$$J^T(\pi^\star) - J^T(\hat{\pi}_f) \leq O\left(\frac{C_f}{\alpha_f} \frac{N^S + N^T}{N^S/\gamma_f + N^T} H^2\left(\sqrt{c}\left(\frac{\log|\Pi|/\delta}{N^T + N^S}\right)^{1/4} + \sqrt{\epsilon_{\text{approx}}}\right) + \frac{\epsilon}{\alpha_f} H^2\right). \quad (E.3)$$

Define

$$L(\hat{\pi}) = \mathbb{E}_{s \sim d^{mix}, g \sim P^T_{\beta,\beta_T}(\cdot|s)}\left[D_{\text{KL}}\left(\pi_f(\cdot|s)||\hat{\pi}(\cdot|s, g)\right)\right].$$

To prove Theorem E.5, we first prove the following result.

Theorem E.6. Consider any function $f : \mathcal{S} \to \mathbb{R}$ such that the assumptions in Assumption E.2 hold. Then for any estimated RCSL policy $\hat{\pi}$ that conditions on f at test time (denoted by $\hat{\pi}_f$), we have

$$J^T(\pi_f) - J^T(\hat{\pi}_f) \leq \frac{C_f\gamma_f}{\alpha_f} H^2\sqrt{2L(\hat{\pi})}.$$

Proof. By definition and Lemma A.2, we have

$$J^T(\pi_f) - J^T(\hat{\pi}_f) = H\left(\mathbb{E}_{P^T_{\pi_f}}[r(s, a)] - \mathbb{E}_{P^T_{\hat{\pi}_f}}[r(s, a)]\right)$$

$$\leq H \cdot \|d_{\pi_f} - d_{\hat{\pi}_f}\|_1$$

$$\leq 2 \cdot \mathbb{E}_{s \sim d^T_{\pi_f}}\left[TV(\pi_f(\cdot|s)||\hat{\pi}_f(\cdot|s))\right]H^2.$$

Next, we have

$$2 \cdot \mathbb{E}_{s \sim d^T_{\pi_f}}\left[TV(\pi_f(\cdot|s)||\hat{\pi}_f(\cdot|s))\right]$$

$$= \mathbb{E}_{s \sim d^T_{\pi_f}}\left[\int_a \left|\pi_f(a|s) - \hat{\pi}_f(\cdot|s)\right|da\right]$$

$$= \mathbb{E}_{s \sim d^T_{\pi_f}}\left[\frac{P^T_{\beta,\beta_T}(\cdot|s)}{P^T_{\beta,\beta_T}(\cdot|s)}\int_a \left|\pi_f(a|s) - \hat{\pi}_f(\cdot|s)\right|da\right]$$

$$\leq 2\frac{C_f}{\alpha_f}\mathbb{E}_{s \sim d^T_{\beta_T}, g \sim P^T_{\beta,\beta_T}(\cdot|s)}\left[TV(\pi_f(\cdot|s)||\hat{\pi}_f(\cdot|s))\right]$$

$$\leq 2\frac{C_f}{\alpha_f}\frac{N^S + N^T}{N^S/\gamma_f + N^T} \cdot \mathbb{E}_{s \sim d^{mix}, g \sim P^T_{\beta,\beta_T}(\cdot|s)}\left[TV(\pi_f(\cdot|s)||\hat{\pi}_f(\cdot|s))\right]$$

$$\leq \frac{C_f}{\alpha_f}\frac{N^S + N^T}{N^S/\gamma_f + N^T} \cdot \mathbb{E}_{s \sim d^{mix}, g \sim P^T_{\beta,\beta_T}(\cdot|s)}\left[\sqrt{2KL(\pi_f(\cdot|s)||\hat{\pi}_f(\cdot|s))}\right]$$

$$\leq \frac{C_f}{\alpha_f}\frac{N^S + N^T}{N^S/\gamma_f + N^T}\sqrt{2L(\hat{\pi})}.$$

$\square$

Proof of Theorem E.5. Following the same argument in the proof of Corollary 3 in Brandfonbrener et al. (2022), we have

$$J^T(\pi_f) - J^T(\hat{\pi}_f) \leq O\Big(2\frac{C_f}{\alpha_f}\frac{N^S + N^T}{N^S/\gamma_f + N^T}H^2\Big(\sqrt{c}\Big(\frac{\log|\Pi|/\delta}{N^S + N^T}\Big)^{1/4} + \sqrt{\epsilon_{\text{approx}}}\Big)\Big).$$

Invoking Theorem E.4, we have

$$J^T(\pi^\star) - J^T(\hat{\pi}_f) \leq O\Big(2\frac{C_f}{\alpha_f}\frac{N^S + N^T}{N^S/\gamma_f + N^T}H^2\Big(\sqrt{c}\Big(\frac{\log|\Pi|/\delta}{N^T + N^S}\Big)^{1/4} + \sqrt{\epsilon_{\text{approx}}}\Big) + \frac{\epsilon}{\alpha_f}H^2\Big).$$

This completes the proof. $\square$